NASA MEMO 4-21-59E

NASA

MEMORANDUM

ANALYSIS OF FLOW-SYSTEM STARTING DYNAMICS OF TURBOPUMP-FED LIQUID-PROPELLANT ROCKET

By Richard P. Krebs and Clint E. Hart

Lewis Research Center
Cleveland, Ohio

NATIONAL AERONAUTICS AND SPACE ADMINISTRATION
WASHINGTON
April 1959

NATIONAL AERONAUTICS AND SPACE ADMINISTRATION

MEMORANDUM 4-21-59E

ANALYSIS OF FLOW-SYSTEM STARTING DYNAMICS OF TURBOPUMP-FED LIQUID-PROPELLANT ROCKET

By Richard P. Krebs and Clint E. Hart

SUMMARY

Two rocket configurations with turbopump drive were investigated analytically. In one configuration the inlet pressure to the turbine was fixed at the design value. The second configuration employed a "bootstrap" technique for supplying energy to the turbine. An injector was the chief resistance between the pump and the rocket combustion chamber.

From the analysis two parameters were developed from which the speed response time of the turbopump, the flow response time, and the maximum dynamic line loss could be evaluated. These parameters were functions of turbopump moment of inertia, design performance of the turbine, and flow-system geometry. The moment of inertia of the turbopump and the ratio of turbine torque at zero speed to design torque had the most influence on the starting dynamics of the flow system. These parameters were also applicable to the bootstrap configuration as long as the inlet pressure to the turbine exceeded half the design value.

INTRODUCTION

The successful firing of a liquid-propellant rocket depends on the proper functioning of its many components. The first few seconds of the launching are extremely critical. During this period the rapidly changing propellant flow rates pyramid difficulties on top of those encountered in the steady-state operation of the rocket. At the Lewis Research Center an analytical study has been made of one phase of the rocket starting problem. This study has been concerned with the flow dynamics involved in rapidly increasing the flow from a value just sufficient to maintain combustion to a value corresponding to that required for full thrust. In this study an attempt has been made to derive information which may be applied to a whole class of rocket flow systems rather than to just a single system.

The initial results of this study are presented in reference 1. In that paper the pump speed is held constant, and the flow dynamics are found to depend primarily on the time history of the main-flow-valve resistance. The present report discusses two new configurations that have been studied. These differ from the original flow system in that the main-flow and bypass control valves have been eliminated and the constant-speed pump has been replaced by a gas generator and turbopump. The flow, speed, torque, and inertia relations of the turbopump are included in the analysis. For the first configuration the turbine-inlet pressure was held constant. A "bootstrap" technique was employed in the second configuration.

The differential equations describing the flow dynamics and the flow, speed, torque, and inertia relations of the turbopump were simulated on an electronic analog computer. The results of the computer study were time histories of the turbopump speed, propellant flow, and dynamic line loss on the suction side of the pump. The effect of changes in system parameters on these quantities is discussed. Generalized parameters, which permit a quick and fairly accurate evaluation of speed and flow response times as well as the maximum dynamic line loss, are developed. Dynamic line loss, as used in this report, is the loss in head between the tank and the suction side of the pump caused by the acceleration of the fluid in the suction line and the friction losses accompanying the flow.

CONFIGURATIONS AND ASSUMPTIONS

The first configuration used in this analysis is shown in figure 1. The configuration represents the essential parts of the flow system of an RP-fuel - liquid-oxygen rocket. This flow system consists of a pressurized propellant tank, a suction line, a centrifugal pump, a discharge line, an injector, and the rocket combustion chamber. The pump is driven by a turbine, and a gas generator supplies the energy for the turbine in the form of hot gases at constant temperature and pressure. The gas generator burns propellants fed from pressurized gas-generator supply tanks.

In analyzing the performance of this rocket configuration, it is assumed that at the beginning of the starting transient the turbopump is windmilling because of the propellant flow from the main pressurized tank through the pump. The propellant flow and turbopump speed are constant, and the pump torque required is zero. At time $t = 0$ a blast of hot gas at design temperature and pressure is supplied to the turbine by the gas generator. The turbopump accelerates and propellant flow increases until the design steady-state conditions are reached.

The bootstrap configuration, shown in figure 2, is similar to the first configuration. Its operation differs from the first configuration in that propellant for the gas generator comes from the gas-generator supply tank for only a short time, and then the gas-generator propellant is bled from the discharge side of the pump through a pressure-reducing valve and a check valve. Such an arrangement makes it possible to use a smaller and lighter gas-generator supply tank.

The bootstrap configuration is assumed to operate in the following manner: At time $t = 0$ the turbopump is windmilling and the turbine is subjected to a blast of hot gas. This time, however, the gas-generator supply-tank pressure is less than the turbine-inlet design pressure, and thus the propellant flow to the gas generator is less than design flow. In the analog-computer representation of this configuration, as the turbopump accelerates, the computer calculates how much propellant would flow through the main gas-generator feed line if check valve B were open. When this calculated flow equals the flow from the pressurized gas-generator supply tank, check valve A closes and check valve B opens. Then the gas-generator pressure becomes a function of the pump pressure. After this switch the turbine continues to accelerate with an increasing turbine-inlet pressure until design conditions are reached.

The assumed pump characteristics are shown in figure 3. These characteristics are for a centrifugal pump and have been generalized over the entire range of speed, flow, head, and efficiency. The curves show m_p/n^2 and h_p/n^2 plotted against q_p/n. (Symbols are defined in appendix A.) The variables m_p, h_p, n, and q_p are dimensionless pump torque, pump head, speed, and flow, respectively. Thus, the variables are actual values divided by design or rated values. The data for these curves were taken from reference 2. These generalized characteristics have been transformed by cross-plotting into the more conventional type of pump map shown in figure 4. In this figure pump head is plotted against flow for various lines of constant speed. Lines of constant efficiency ratio are also shown.

For most of this analysis a two-stage turbine was assumed. The torque-speed relations were calculated for several turbine-inlet pressures from reference 3. For these calculations the turbine-inlet temperature was assumed fixed, and the turbine was assumed to exhaust through a suitable convergent nozzle to the atmosphere. The results are plotted in figure 5 in terms of fraction of design turbine torque m_t, fraction of design speed n, and ratio of turbine-inlet pressure to design turbine-inlet pressure h_g.

It was assumed that these characteristics could be represented by the equation

$$m_t = h_g[r - (r - 1)n] \qquad (1)$$

where r is the ratio of the turbine torque at zero speed to the torque at rated speed. Torque-speed lines computed from equation (1) for $r = 1.8$ and several values of h_g are also shown in figure 5. The straight-line assumptions for turbine torque based on equation (1) are good for turbine-inlet pressures greater than 0.5 design, but at lower inlet pressures the torque is appreciably greater than that calculated from reference 3. At 0.8 design speed and 0.2 design inlet pressure the torque from equation (1) is 31 percent greater than the torque calculated from reference 3.

Assumed torque-speed characteristics for four different two-stage turbine designs are shown in figure 6. These designs differ in the degree of criticalness, that is, the ratio of speed to stage work (ref. 3). Similar characteristics could also be obtained with a single-stage turbine with a reduction in moment of inertia and an increase in mass-flow rate.

The components of both flow-system configurations described herein were sized to be representative of an RP-fuel - liquid-oxygen rocket system delivering approximately 300,000 pounds of thrust. Design values for the system components are given in table I.

SYSTEM EQUATIONS AND ANALOG-COMPUTER SIMULATION

The basic equations for the configuration shown in figure 1 are essentially the same as those derived in reference 1. The head at the discharge side of the pump is equal to the sum of the head in the rocket chamber, the loss in head across the injector, and the head needed to accelerate the fluid and to overcome friction in the discharge line, minus the elevation head of the discharge line:

$$H_4 = GQ_p + R_c Q_p^2 + \frac{L_d}{gA_f}\dot{Q}_p + \frac{fL_d}{2gDA_f^2} Q_p^2 - H_{de} \tag{2}$$

The head at the suction side of the pump is equal to the tank head plus the elevation head of the suction line minus the head needed to accelerate the fluid and to overcome friction in the suction line:

$$H_3 = H_1 + H_{se} - \frac{L_s}{gA_f}\dot{Q}_p - \frac{fL_s}{2gDA_f^2} Q_p \tag{3}$$

The last two terms of this equation represent the dynamic line loss H_{sl}. The head rise across the pump H_p is equal to the difference between H_4 and H_3:

$$H_p = GQ_p + \left[R_c + \frac{f(L_s + L_d)}{2gDA_f^2}\right]Q_p^2 + \frac{L_s + L_d}{gA_f}\dot{Q}_p - H_1 - H_{se} - H_{de} \qquad (4)$$

Since in this analysis the dynamic response of the turbopump is included, the following torque balance equation is needed:

$$M_t - M_p = \frac{\pi}{30} I\dot{N}_t \qquad (5)$$

Also needed for this analysis are curves relating head, torque, flow and speed for the pump, and torque and speed for the turbine. The generalized curves shown in figures 3 and 5 or 6 are well suited for this analog-computer simulation.

In preparing a block diagram for the configuration, equation (4) was solved for $\dot{Q}_p$, letting K_I equal the coefficient of $\dot{Q}_p$ and K_R equal the coefficient of Q_p^2:

$$\dot{Q}_p = \frac{H_p}{K_I} + \frac{1}{K_I}(H_1 + H_{se} + H_{de}) - \frac{K_R}{K_I}Q_p^2 - \frac{G}{K_I}Q_p \qquad (6)$$

Equations (5) and (6) and the pump and turbine curves of figures 3 and 5 or 6 are represented by the solid-line portion of figure 7. The various analog-computer components were interconnected as indicated by this block diagram. Time and amplitude scale factors were determined from the expected magnitude and frequency range of the system dependent variables.

Analog-computer solutions consisting of time histories of turbopump speed, propellant flow, pump head, and dynamic line loss were obtained for various values of turbopump moment of inertia, turbine zero-speed torque ratio, and rocket chamber pressure. In each case the initial values of turbopump speed and propellant flow were chosen so that required pump torque was zero and propellant flow was constant (i.e., $\dot{Q}_p = 0$).

For the bootstrap configuration (fig. 2) another equation is needed to describe the flow conditions in the main gas-generator feed line. This equation is

$$G_g Q_g = H_4 - R_v Q_g^2 - \frac{L_g}{gA_g}\dot{Q}_g \qquad (7)$$

Friction losses in the feed line were neglected. In equation (7) the term H_4 can be replaced by $H_3 + H_p$. Then by using equation (3) H_3 can be eliminated, and solving for $\dot{Q}_g$ the following equation can be obtained:

$$\dot{Q}_g = \frac{H_1 + H_{se}}{K_g} - \frac{H_{sl}}{K_g} + \frac{H_p}{K_g} - \frac{G_g}{K_g} Q_g - \frac{R_v}{K_g} Q_g^2 \qquad (8)$$

where K_g is the coefficient of $\dot{Q}_g$ in equation (7).

Equation (8) is represented by the dotted portion of figure 7. A comparator and a switching device are also shown in figure 7. They are needed to represent the valve operations in the gas-generator feed lines during the bootstrap starting operation. The comparator determines when a calculated propellant flow through the gas-generator feed line from the pump would be equal to the actual flow from the pressurized gas-generator supply tank. When the calculated flow and the actual flow are equal, the comparator actuates the switching device and the propellant flow to the gas generator no longer comes from the supply tank but from the pump and is a function of the pump outlet head for the remainder of the transient. Analog-computer solutions were obtained for the bootstrap configuration covering a range of initial turbine-inlet pressures from 10 to 100 percent of the design value.

RESULTS

Analog-computer traces for a starting transient of the first configuration are shown in figure 8. Fractions of rated flow q_p, speed n, and pump head h_p, and the dynamic line loss H_{sl} were recorded as functions of time in figure 8(a). The dynamic line loss was also recorded on rectinlinear coordinates as a function of time (fig. 8(b)). On both figures increasing dynamic line loss (decreasing head at the pump inlet) is in the downward direction. These particular traces are for the nominal configuration with a turbopump moment of inertia I of 0.28 (lb)(ft)(sec^2) and a turbine zero-speed torque ratio r of 1.8.

For the nominal configuration the maximum dynamic line loss was 25 feet, and the speed and flow response times were 0.22 and 0.28 second, respectively. Response time is defined as the time required for a variable (in this case, speed or flow) to execute 63.2 percent, or $1 - 1/e$, of its total transient change.

The initial values of flow and speed for the nominal configuration were computed from equation (6). At the start of the transient both the

pump flow and speed are constant so that $\dot{Q}_p = 0$. Furthermore, because the pump is windmilling, the pump torque and m_p are zero. If the substitutions $H_p = H_p' h_p$, $Q_p = Q_p' q_p$, and $\dot{Q}_p = 0$ are introduced into equation (6), it becomes

$$H_p' \frac{h_p}{q_p^2} q_p^2 + (H_1 + H_{se} + H_{de}) - K_R (Q_p')^2 q_p^2 - G Q_p' \dot{q}_p = 0 \qquad (9)$$

Reference to figure 3 shows that when m_p is zero ($m_p/n^2 = 0$), $q_p/n = 3$, and $h_p/n^2 = -2$. Using these values, equation (9) can be solved for the initial value of flow to give $q_{p,0} = 0.075$. The corresponding value for n_0 is 0.025.

Effect of Changes in Turbopump Moment of Inertia

The effect of changes in the turbopump moment of inertia on the dynamics of the propellant flow system was studied by varying the moment of inertia from about twice its nominal value of 0.28 (lb)(ft)(sec^2) to about 0.1 its nominal value. For this part of the analysis the zero-speed torque ratio of the turbine was held at a value of 1.8. The results are shown in figures 9 and 10. In figure 9 the flow response time and speed response time are plotted against the fraction of design moment of inertia. Both flow and speed response times increase linearly with an increase in moment of inertia. The flow response is slower than the speed response because, in the case of the flow, it is necessary to accelerate the mass of the fluid as well as the rotating mass of the turbopump.

Figure 10 shows the effect of changes in turbopump moment of inertia on the maximum value of the dynamic line loss and the time at which it occurs. The dynamic line loss is proportional to the rate of change of flow if the friction loss is small compared with the acceleration loss (see eq. (3)). The maximum dynamic line loss, therefore, coincides in time with the maximum slope of the flow-time curve. Like the flow and speed response times, the time at which the dynamic line loss is a maximum increases nearly linearly with the turbopump moment of inertia. The higher flow response times which are encountered as the moment of inertia is increased bring about decreased values of maximum dynamic line loss. With a turbopump moment of inertia twice the design value the maximum dynamic line loss was about 12 feet and occurred about 0.26 second after the starting transient was initiated. With a turbopump moment of inertia one-half that at design the maximum dynamic line loss was 51 feet and occurred at 0.06 second after starting.

From the foregoing discussion it can be seen that a decrease in turbopump moment of inertia is desirable to produce a rapid flow response. On the other hand, decreasing the moment of inertia gives rise to high dynamic line losses. Too low a moment of inertia may produce such a large dynamic line loss that the pump may cavitate and suffer a serious loss in performance.

The minimum suction head H_{sv} required to prevent cavitation is related to the suction specific speed S, flow Q_p, and actual speed N_p through the relation

$$H_{sv} = \left(\frac{21.185\ N_p\sqrt{Q_p}}{S}\right)^{4/3} \tag{10}$$

The pump in this analysis was designed for a suction specific speed of 30,000, which is typical of some contemporary high-performance pumps. In order to calculate H_{sv}, it is necessary to know the relation between flow and speed during the transient. In figure 11 dimensionless flow is plotted against dimensionless speed for the nominal design configuration. The minimum suction head required to prevent cavitation was calculated by means of equation (10) using the flow-speed relation shown in figure 11 and a value of 30,000 for suction specific speed. The results are shown in figure 12, where required suction head H_{sv} is plotted against fraction of design speed n. This curve can be shown to be practically independent of moment of inertia.

The available suction head at the pump inlet H_3 for the nominal value of moment of inertia is also plotted in figure 12. This head was computed by subtracting the dynamic line loss, occurring during a starting transient, from an available static head of 80 feet (above vapor pressure) at the pump inlet. The static head was made up of the pressurization (above vapor pressure) in the tank equivalent to 40 feet of liquid propellant, 20 feet of liquid in the tank, and a 20-foot column of liquid in the suction line. The lower curve in figure 12 shows that the suction head required is less than 5 feet for fractions of design speed up to 0.4. This means that the dynamic line loss, if it occurs at pump speeds less than 0.4 design, can absorb all but 5 feet of the static head before cavitation sets in. For the nominal case ($I = 0.28$ (lb)(ft)(sec^2), $r = 1.8$), plotted in figure 12, the maximum dynamic line loss occurs at a speed of about 0.4 rated, and the available suction head is about 50 feet greater than the required suction head. Because the speed response time and the time for the occurrence of the maximum dynamic line loss are both proportional to I (figs. 9 and 10), there is a constant ratio between the two times. This constant ratio implies that the maximum dynamic line loss will occur at the same fraction of design speed n so long as there is no significant change in the shape of the speed-time curve.

Effect of Turbine Torque-Speed Relation

The relation between turbine torque and turbine speed is a function of turbine design. The torque at zero speed may be increased or decreased, while the torque at design speed remains constant, by changing the number of turbine stages, or changing the criticalness of design, or both.

A turbine with each of the torque-speed characteristics shown in figure 6 was used in turn in the analog-computer study. The results of changes in the torque-speed relation are shown in figure 13, where flow and speed response times are plotted as functions of zero-speed torque ratio r. Increasing the torque at zero speed from 1.2 to 1.8 times design torque decreased the speed response time from 0.30 to 0.22 second. A similar decrease in flow response time occurred.

In figure 14 the magnitude and the time of the maximum dynamic line loss are plotted as functions of the zero-speed torque ratio. The data show that as the torque at zero speed increased from 1.2 to 1.8 times design torque, the maximum dynamic line loss increased from 18 to 25 feet and the time decreased from 0.19 to 0.13 second.

Effect of Simultaneous Change in Turbopump Moment of Inertia and Turbine Torque-Speed Relation

The results of the last two sections have been based upon the assumption of a two-stage turbine in the turbopump. By means of reference 3 it is possible to calculate the performance of a single-stage turbine assuming the same design inlet and outlet pressures as the preceding two-stage turbine. For a single-stage turbine, the torque at zero speed was calculated from reference 3 to be 1.3 times design torque. The single-stage turbine was assumed to have one-half the rotating mass of the two-stage turbine with a consequent reduction in turbopump moment of inertia from 0.28 to 0.176 $(lb)(ft)(sec^2)$. The simultaneous reduction in zero-speed torque and moment of inertia decreased the speed response time from 0.22 to 0.18 second and increased the maximum dynamic line loss from 25 to 31 feet.

Moment of Inertia and Torque Generalization

Speed response. - In order to correlate the effects of changes in turbopump moment of inertia and zero-speed turbine torque, described in the preceding three sections, an approximate analysis of the starting dynamics of the turbopump was made. For this approximate analysis the torque developed by the turbine and the torque required by the pump were

compared in the low-speed range. The two fractional torques are plotted against fraction of design speed for the nominal configuration in figure 15. For speeds up to 0.632 design speed, the pump torque is less than 30 percent of the turbine torque, and the ratio of the areas under the two curves from $n = 0$ to $n = 0.632$ is less than 0.09. As a consequence, for low speeds it seemed permissible to neglect the torque required by the pump as compared with the torque delivered by the turbine.

In appendix B this assumption is used in deriving a turbopump speed response parameter. This turbopump speed response parameter T is equal to the response time of the turbopump, assuming zero idling speed and no torque requirement for the pump, and is given by

$$T = \frac{\pi I N_t'}{30 M_t' h g (r - 1)} \ln \frac{r}{0.368\ r + 0.632} \tag{11}$$

Equation (11) shows that T is directly proportional to I, and reference to equation (5) and figure 9 shows that the time required to reach any speed, including the response time, is also proportional to I.

Because the torque required by the pump has been neglected, the turbopump speed response parameter will not equal the speed response time, and the difference between the two will depend on the relative magnitudes of the turbine and pump torques. In this analysis the pump torque-speed relation is fixed, and only the turbine torque can be changed; that is, by varying the zero-speed torque parameter r. The difference between the turbopump speed response time and the turbopump speed response parameter is illustrated in figure 16, where time is plotted against the parameter. The data are for a two-stage turbine with $I = 0.28$ and values of r between 1.2 and 2.0, and for a single-stage turbine. A 45° line corresponding to equality of the two quantities is also shown for comparison. The speed response time is about 12 percent greater than the turbopump speed response parameter over the range of r investigated.

Since the assumed pump and turbine torques are typical of those found in a turbopump, it may be concluded that the speed response time of a turbopump will be from 10 to 15 percent greater than the value of the parameter T. This parameter is evaluated from readily determined quantities, such as design turbine speed, turbine torque at zero and design speed, and turbopump moment of inertia.

Flow response. - Because the propellant flow rate is one of the most important factors in determining the thrust of a rocket, some simple means of evaluating flow response time might be of value. Flow and speed response times are plotted against moment of inertia and zero-speed torque ratio in figures 9 and 13, respectively. Over a large range of moments of inertia and torque ratios the flow response time was about 30 percent larger than the speed response time. Numerical solutions for the equations given in the section SYSTEM EQUATIONS AND ANALOG-COMPUTER SIMULATION for several values of r and I failed to show any

consistent variation in the ratio of flow response time to speed response time with changes in r and I.

Maximum dynamic line loss. - To attempt to correlate the effects of changes in turbopump moment of inertia and zero-speed torque ratio on the maximum dynamic line loss it was assumed that the maximum dynamic loss could be written as some constant times the dynamic-line-loss parameter U:

$$\text{Maximum dynamic line loss} = KU = K\left(\frac{L_s Q_p'}{gA_f T}\right) \tag{12}$$

The parameter $U = L_s Q_p'/gA_f T$ is developed in appendix C.

The maximum dynamic line loss, as obtained from analog-computer traces, was plotted against the dynamic-line-loss parameter with the results shown in figure 17. Data are included for a range of I and r. The correlation between the maximum loss and the parameter is good, and the constant of proportionality K is about 0.57.

By use of equations (11) and (12) relations were established between the moment of inertia I and the zero-speed torque ratio r for particular values of dynamic line loss. These relations are plotted in figure 18. With the help of this figure, limits can be set on either I or r for any allowable value of maximum dynamic line loss. For example, for the configuration illustrated in figure 1, a maximum dynamic line loss of 75 feet can be tolerated (fig. 12). With a nominal value for the zero-speed torque ratio of 1.8 it would be permissible to lower the turbopump moment of inertia to about 0.1 (lb)(ft)(sec^2) before the head at the pump inlet would fall sufficiently to cause cavitation.

Effect of Changes in Combustion-Chamber Pressure

The combustion stability of a rocket may be improved (refs. 4 to 6) or the design thrust may be altered by a change in the combustion-chamber pressure. The effect on flow-system dynamics was studied by changing the combustion-chamber pressure through an appropriate change in the injector pressure drop, while the design pump head was held constant. The results are shown in figure 19, where speed and flow response times are plotted against design combustion-chamber pressure. Both response times remained virtually constant over the range of pressures investigated.

Effect of Changes in Pump Characteristics

The effect of changes in pump design was not specifically investigated on the analog. However, if the magnitude of the design pump head is fixed, then changes in pump design can affect only the torque and head curves of figure 3, or the turbopump moment of inertia I, or both.

Because the pump torque at low speeds is small, and because it was neglected in deriving the turbopump speed parameter T and in establishing the correlation between T and the speed response time, small changes in the low-speed torque characteristics should not disturb the correlation found by this analysis. At rated speed all pumps would have power requirements which matched the turbine power capabilities.

The head curve in figure 3 could be lowered for values of q_p/n less than unity, for example, by decreasing the amount of sweepback on the impeller blades. If more nearly radial blades were assumed, the head curve of figure 3 would be more nearly flat at a value of 1.0 for values of q_p/n less than 1.0, and the biggest difference in the two curves would be at low values of q_p/n. However, in the configuration analyzed the minimum value of q_p/n encountered was 0.62, as shown in figure 20. This figure shows that, initially, the speed n is 0.025 rated and q_p/n has a value of 3.0. As the speed increases, q_p/n rapidly decreases until, at a value of $n = 0.2$, q_p/n has reached its minimum value of about 0.62. As the speed increases further, both n and q_p/n asymptotically approach 1.0. At $q_p/n = 0.62$ the value of h_p/n^2 is about 1.15 in figure 3. This means that the instantaneous head rise on a pump with a flat head-speed characteristic would differ from the value used in the analysis by no more than 15 percent during the starting transient. Such a change would not show up in the speed response, but might tend to increase the flow response time.

Therefore, it is concluded that, if the design head on the pump is held fixed, changes in pump design will affect the speed response time and speed response parameter chiefly through changes in moment of inertia, and that the change in the ratio of flow response time to speed response time will be small.

Bootstrap Configuration

For the analog study of the bootstrap configuration, nominal design values of turbopump moment of inertia and turbine zero-speed torque ratio were used. The initial turbine-inlet pressure ratio h_g was varied from 0.1 to 1.0 to determine the effect on starting dynamics. Figure 21 shows the dynamic line loss as a function of time for several values of h_g. The zero or starting point for each curve was shifted on the recorder to separate the curves. The breaks in the curves (e.g., at $t = 0.43$ sec and $h_g = 0.7$) indicate the switching of the gas-generator propellant source from the constant-pressure supply tank to the pump discharge.

The effects of changes in turbine-inlet pressure ratio h_g on the flow and speed response times are shown in figure 22. Decreasing h_g from 1.0 to 0.1 increased the flow and speed response times to about four times their nominal values.

In figure 23 the magnitude and time of occurrence of the maximum dynamic line loss are plotted against h_g. Both curves show comparatively abrupt changes between $h_g = 0.4$ and $h_g = 0.5$. Portions of the curves are dotted because the exact shape in these regions was not determined. As h_g was decreased the maximum dynamic line loss decreased linearly until h_g reached a value of about 0.4. At this value of h_g the maximum dynamic line loss was about 8.7 feet. It remained at this value as h_g was decreased further. The change in the curve showing time of maximum dynamic line loss was even more abrupt in the region between $h_g = 0.4$ and $h_g = 0.5$.

An explanation for the trends and abrupt changes of the curves can be found by referring to figure 21. For values of h_g of 0.5 and higher, the maximum dynamic line loss occurs before the switch in gas-generator propellant source from the constant-pressure supply tank to the pump discharge. For values of h_g of 0.4 and lower, the maximum dynamic line loss occurs after the switch.

Speed response times for the boostrap configuration are plotted against the turbopump speed response parameter in figure 24. It can be seen that the correlation between speed response time and the speed response parameter is not as good for the bootstrap configuration as it is for the first configuration. For values of h_g from 1.0 to 0.4 the speed response time is up to 25 percent greater than the speed response parameter. For values of h_g less than 0.4 the speed response time varies from 25 percent greater to 50 percent less than the corresponding parameter.

There are two factors which disturb the correlation between speed response time and the parameter in the bootstrap configuration. As the turbine-inlet pressure is decreased from its design value, the turbine torque curve in figure 15 is lowered, and the pump torque is no longer negligible in comparison. As the pump torque becomes relatively more important, the speed response time increases for a given turbopump speed response parameter. This is illustrated in figure 24 for values of h_g from 1.0 to 0.4 where the speed response time rises progressively above the dotted 45° line. The second disturbing factor involves the relative chronology of the switching time and the speed response time. If the switch from constant turbine-inlet pressure to a pressure derived from the pump discharge occurs prior to the speed response time, then the h_g used in determining the turbopump speed response parameter should not be

the h_g determined from the gas-generator supply tanks, but rather an integrated value which would include both the constant h_g and the h_g derived from the pump discharge. The effective h_g is thus higher than the initial h_g. Use of an effective h_g thus would result in a smaller speed response parameter. The effect would be most noticeable at the lowest value of h_g (0.1) in figure 24.

Values of maximum dynamic line loss for the bootstrap configuration are plotted against the dynamic-line-loss parameter in figure 25. The dotted line represents the correlation obtained for the first configuration and was transposed from figure 17. The correlation for the bootstrap configuration is within 12.5 percent for values of h_g of 0.4 to 1.0. For values of h_g less than 0.4 the correlation is poor. Because the dynamic-line-loss parameter is related to the speed response parameter (appendix B), the same factors affect the correlation of both parameters.

CONCLUSIONS

The following conclusions were derived from an analog-computer study of the starting transients in a representative turbopump flow system for a large, liquid-propellant rocket engine. The system consisted of a pressurized propellant tank, a turbopump, an injector, a rocket combustion chamber, a gas generator and supply tank, and lines connecting the various components. There was no control valve in the main propellant feed line. The starting transient was considered from the time when hot gases were first admitted to the turbine until design conditions had been established.

1. Two parameters, involving only the moment of inertia of the turbopump and certain design parameters of the turbine, have been developed which predict the speed response time of the turbopump and the maximum value of the dynamic line loss.

2. The moment of inertia of the turbopump and the ratio of the torque at zero speed to design torque have the most effect on the starting dynamics of the flow system.

3. The turbopump parameter and maximum-dynamic-line-loss parameter may be applied to a bootstrap configuration if the initial turbine-inlet pressure is greater than half the design pressure.

Lewis Research Center
National Aeronautics and Space Administration
Cleveland, Ohio, January 29, 1959

APPENDIX A

SYMBOLS

A_f	cross-sectional area of principal flow-system lines, sq ft
A_g	cross-sectional area of gas-generator supply lines, sq ft
D	diameter, ft
f	friction factor
G	constant of proportionality between propellant flow and chamber head produced by combustion process, (ft)(sec)/cu ft
g	acceleration due to gravity, 32.17 ft/sec^2
H	head, ft
h	fraction of design head
I	turbopump moment of inertia, (lb)(ft)(sec^2)
K, K_I, K_N, K_R	constants
L	length, ft
M	torque, ft-lb
m	fraction of design torque
N	rotational speed, rpm
n	fraction of design speed
Q	volume flow, cu ft/sec
q	fraction of design flow
R	resistance, sec^2/ft^5
r	ratio of turbine torque at zero speed to design turbine torque
S	suction specific speed (see eq. (8))
T	turbopump parameter, sec

t time, sec

U dynamic-line-loss parameter, ft

Subscripts:

a accelerating

c chamber

d discharge line

de discharge-line elevation

g gas generator

p pump

s suction line

se suction-line elevation

sl dynamic loss in suction line

sv net positive suction above vapor pressure

t turbine

v valve

0 value at t = 0

1 tank

3 pump inlet

4 pump discharge

Superscripts:

• derivative with respect to time

' design value

APPENDIX B

DERIVATION OF CORRELATING PARAMETERS

Turbopump Speed Response Parameter

In any piece of rotating machinery the accelerating torque M_a is equal to the product of the moment of inertia of the rotating mass and the time rate of change of the angular velocity:

$$M_a = \frac{\pi I \dot{N}}{30} \tag{B1}$$

In the turbopump the accelerating torque is equal to the difference between the torque developed by the turbine and the torque required by the fuel and oxidant pumps. In accordance with figure 5, the torque developed by the turbine varies linearly with the turbine speed n and with the turbine-inlet pressure ratio h_g, so that

$$M_a = M_t - M_p = h_g M_t'[r - (r - 1)n] - M_p \tag{B2}$$

If the right sides of equations (B1) and (B2) are set equal to each other, the following relation is obtained:

$$\frac{30dt}{\pi I N_t'} = \frac{dn}{h_g M_t'[r - (r - 1)n] - M_p} \tag{B3}$$

This equation can be integrated to yield a functional relation between t and n as soon as M_p is known as a function of n. Equation (B3) shows, among other things, that the time required to pass between fixed limits of n is directly proportional to I.

A turbopump speed response parameter was derived by integrating equation (B3) from $n = 0$ to $n = (1 - 1/e)$, or $n = 0.632$. The pump torque M_p was assumed equal to zero when this integration was carried out. This assumption is valid at low speeds, as shown by figure 15. The resulting integral of dt in equation (B3), under the foregoing assumptions, has been identified as the turbopump speed response parameter T, and

$$T = \frac{\pi I N_t'}{30 M_t' h_g (r - 1)} \ln \frac{r}{0.368\ r + 0.632} \tag{11}$$

It can be seen that even with the simplifying assumptions T varies directly with I, as did the speed response time. However, when the

pump torque is neglected, the effect of h_g and r on the speed response time and the speed response parameter will be different, because h_g and r determine M_t, from which M_p is subtracted.

Dynamic-Line-Loss Parameter

The dynamic line loss is given by

$$H_{sl} = \frac{L_s\dot{Q}_p}{gA_f} + \frac{fL_sQ_p^2}{2gDA_f^2} \tag{B4}$$

(see discussion on eq. (3)). In the present investigation the friction term, or second term, was small compared with the first. This is true in reference 1 also. The first term $L_s\dot{Q}_p/gA_f$ is used as a model from which to construct a dynamic-line-loss parameter. The $\dot{Q}_p$ is replaced by $(Q_p' - Q_{p,0})/T = Q_p'/T$. The resulting dynamic-line-loss parameter becomes $U = L_sQ_p'/gA_fT$.

REFERENCES

1. Krebs, Richard P.: Effect of Fluid-System Parameters on Starting Flow in a Liquid Rocket. NACA TN 4054, 1957.

2. Kittredge, C. P.: Hydraulic Transients in Centrifugal Pump System. Trans. ASME, vol. 78, no. 6, Aug. 1956, pp. 1307-1320; discussion, pp. 1320-1322.

3. Stewart, Warner L.: Torque-Speed Characteristics for High-Specific-Work Turbines. NACA TN 4379, 1958.

4. Summerfield, Martin: A Theory of Unstable Combustion in Liquid Propellant Rocket Systems. Jour. Am. Rocket Soc., vol. 21, no. 5, Sept. 1951, pp. 108-114.

5. Barrere, M., and Moutet, A. L.: Low-Frequency Combustion Instability in Bipropellant Rocket Motors. Jet Prop., vol. 26, no. 1, Jan. 1956, pp. 9-19.

6. Li, Y. T.: Stabilization of Low-Frequency Oscillations of Liquid Propellant Rockets with Fuel Line Stabilizer. Jet Prop., vol. 26, no. 1, Jan. 1956, pp. 26-33; 39.

TABLE I. - NOMINAL DESIGN VALUES OF FLOW-SYSTEM PARAMETERS

Rocket chamber pressure, lb/sq in. gage	480
Injector pressure drop, lb/sq in.	328
Discharge-line length, L_d, ft	2
Suction-line length, L_s, ft	20
Propellant-line area, A_f, sq ft	0.836
Propellant-line friction factor, f	0.025
Propellant (oxygen) flow, Q'_p, cu ft/sec	12
Oxygen pump head rise, H'_p, ft	1630
Oxygen pump speed, N'_p, rpm	7325
Total (oxygen and fuel) pump torque referred to turbine speed, M'_p, ft-lb	1359
Turbine speed, N'_t, rpm	22,250
Turbine torque, M'_t, ft-lb	1359
Turbopump moment of inertia, referred to turbine speed, I, (lb)(ft)(sec^2)	0.28
Propellant-tank static head, H_1, ft	60
Gas-generator propellant (oxygen) flow, Q'_g, cu ft/sec	0.05
Turbine-inlet pressure, lb/sq in. gage	335.3
Gas-generator-line length, L_g, ft	4
Gas-generator-line area, A_g, sq in.	0.4

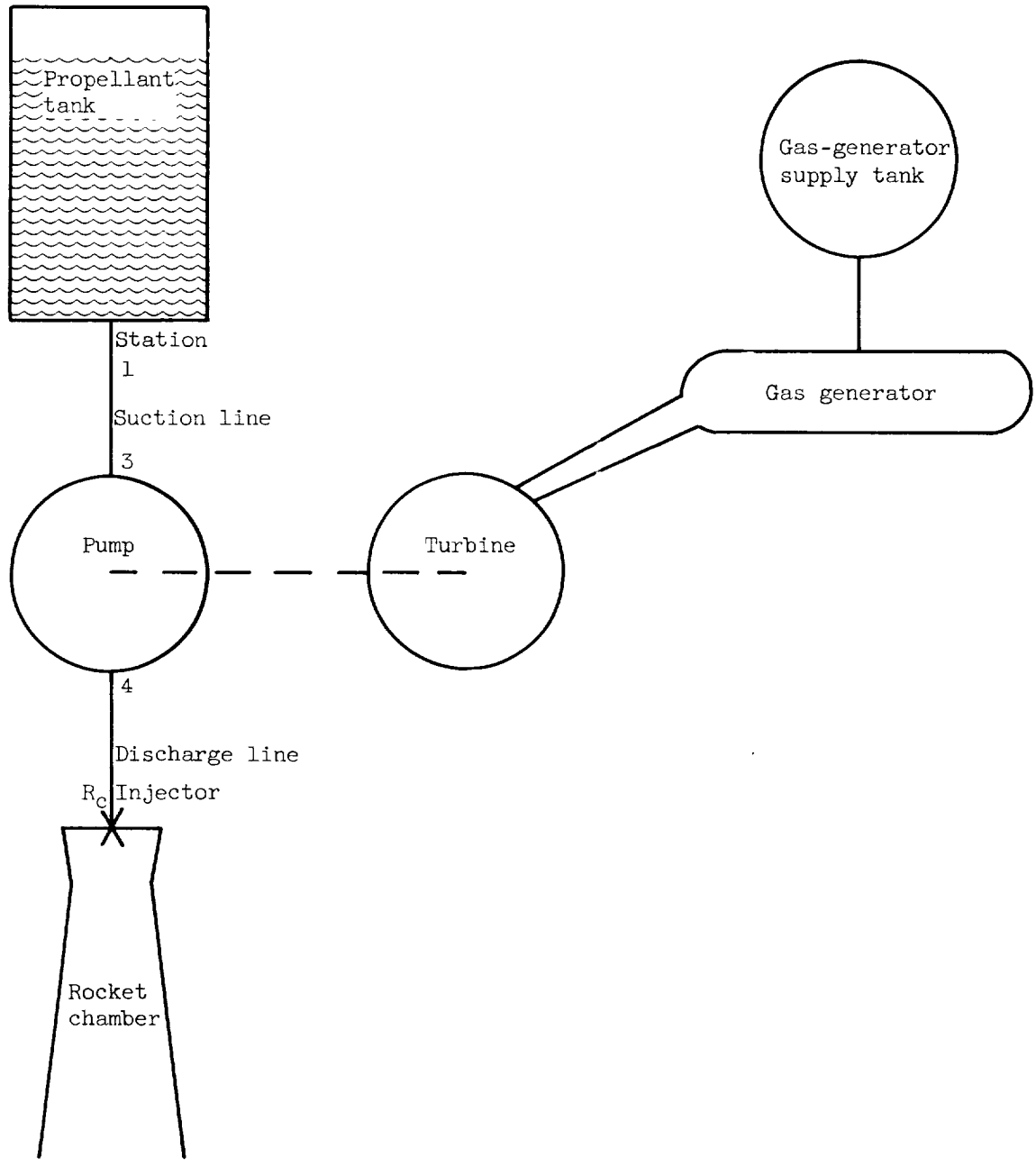

Figure 1. - Schematic diagram of rocket flow system with fixed-pressure turbine drive.

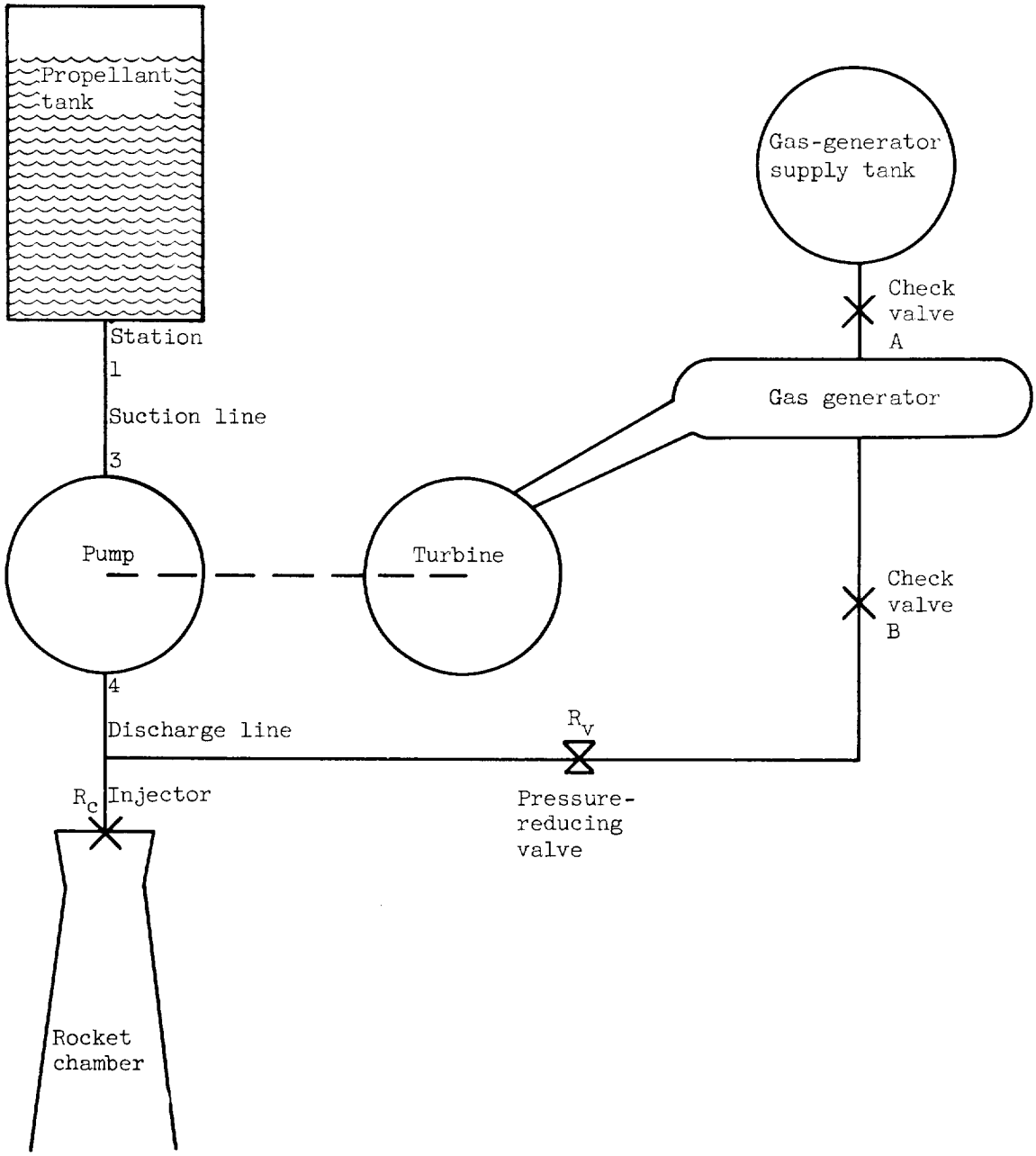

Figure 2. - Schematic diagram of rocket flow system with bootstrap turbine drive.

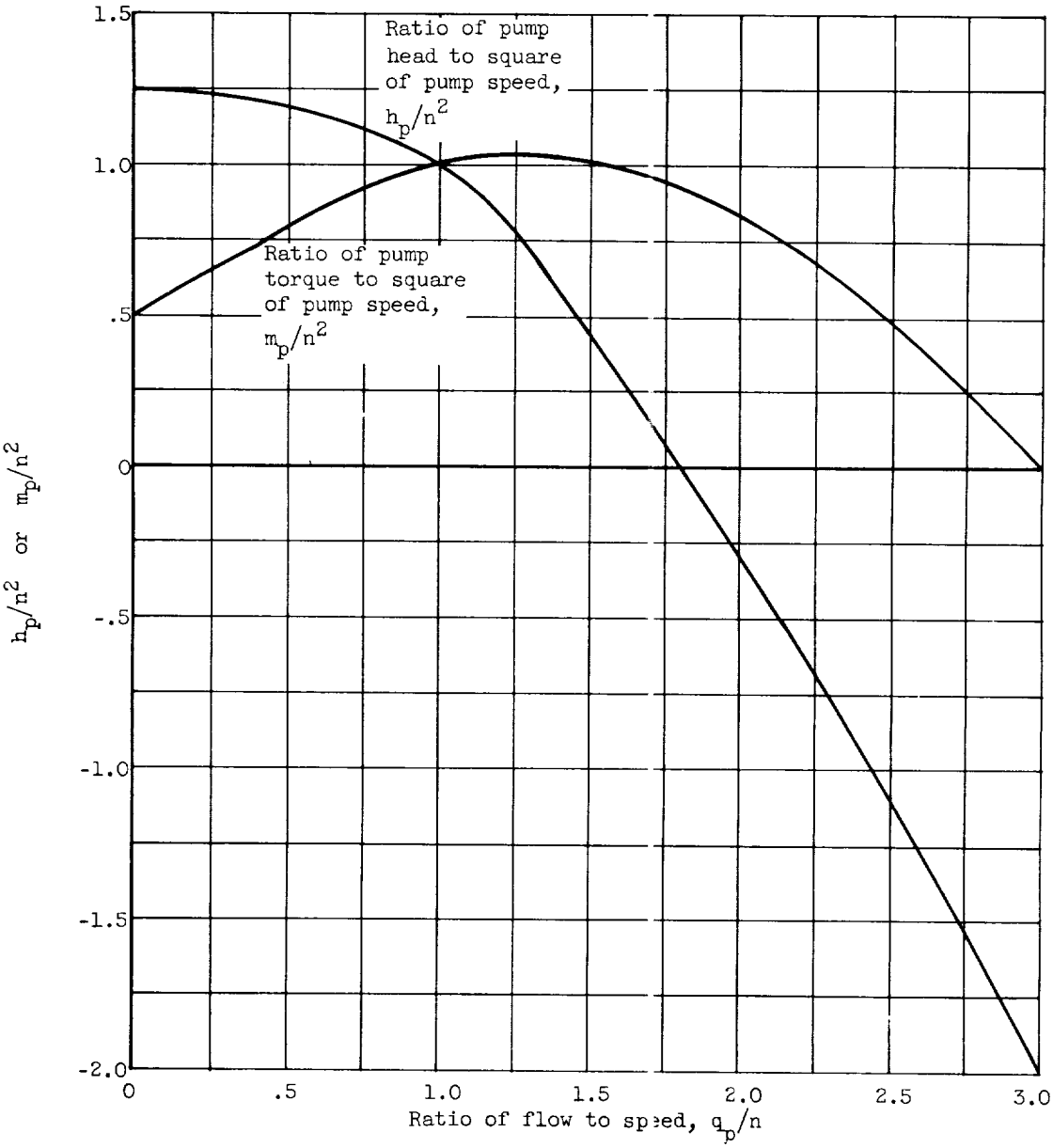

Figure 3. - Assumed pump characteristics derived from reference 2.

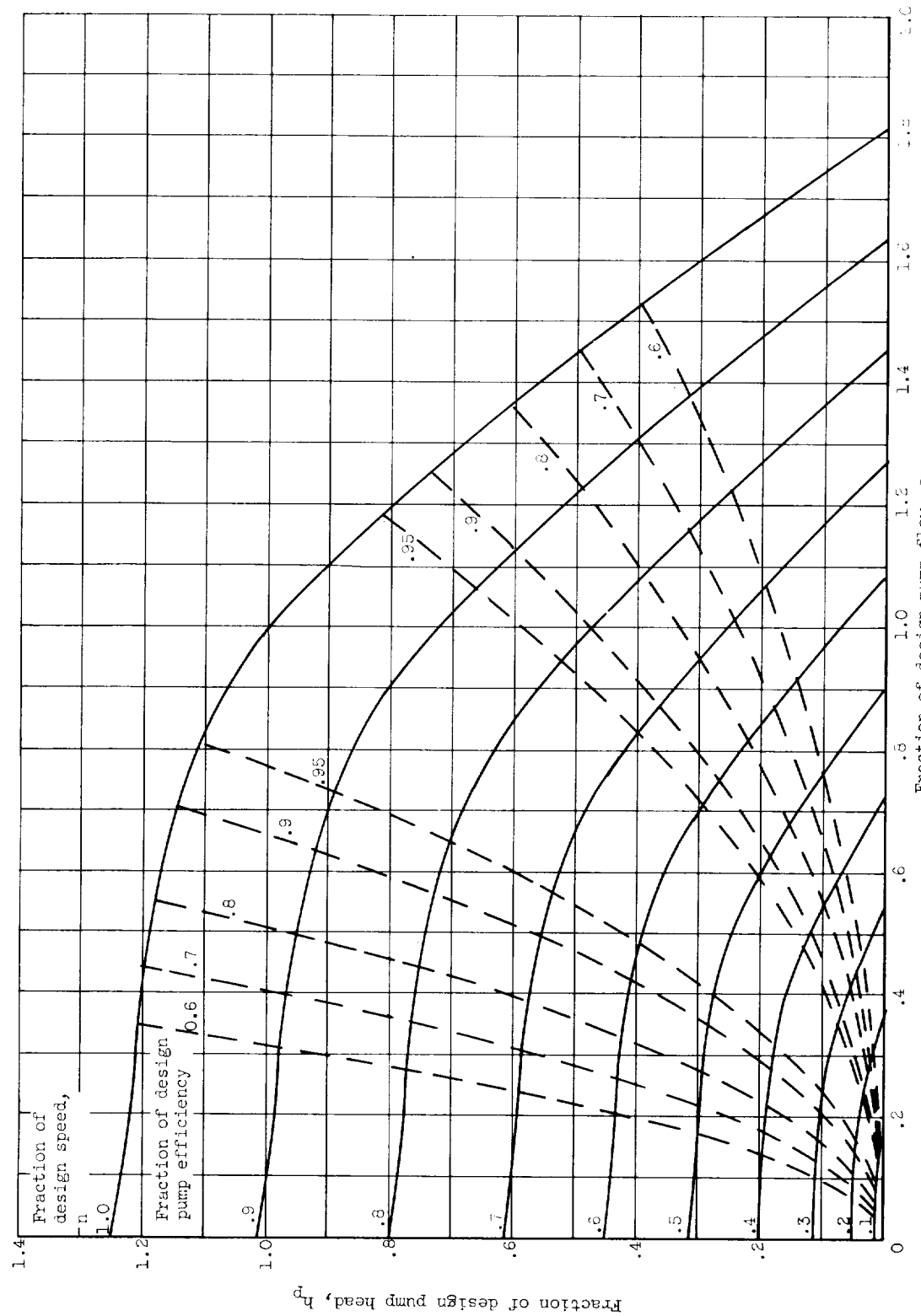

Figure 4. - Conventional presentation of assumed pump characteristics.

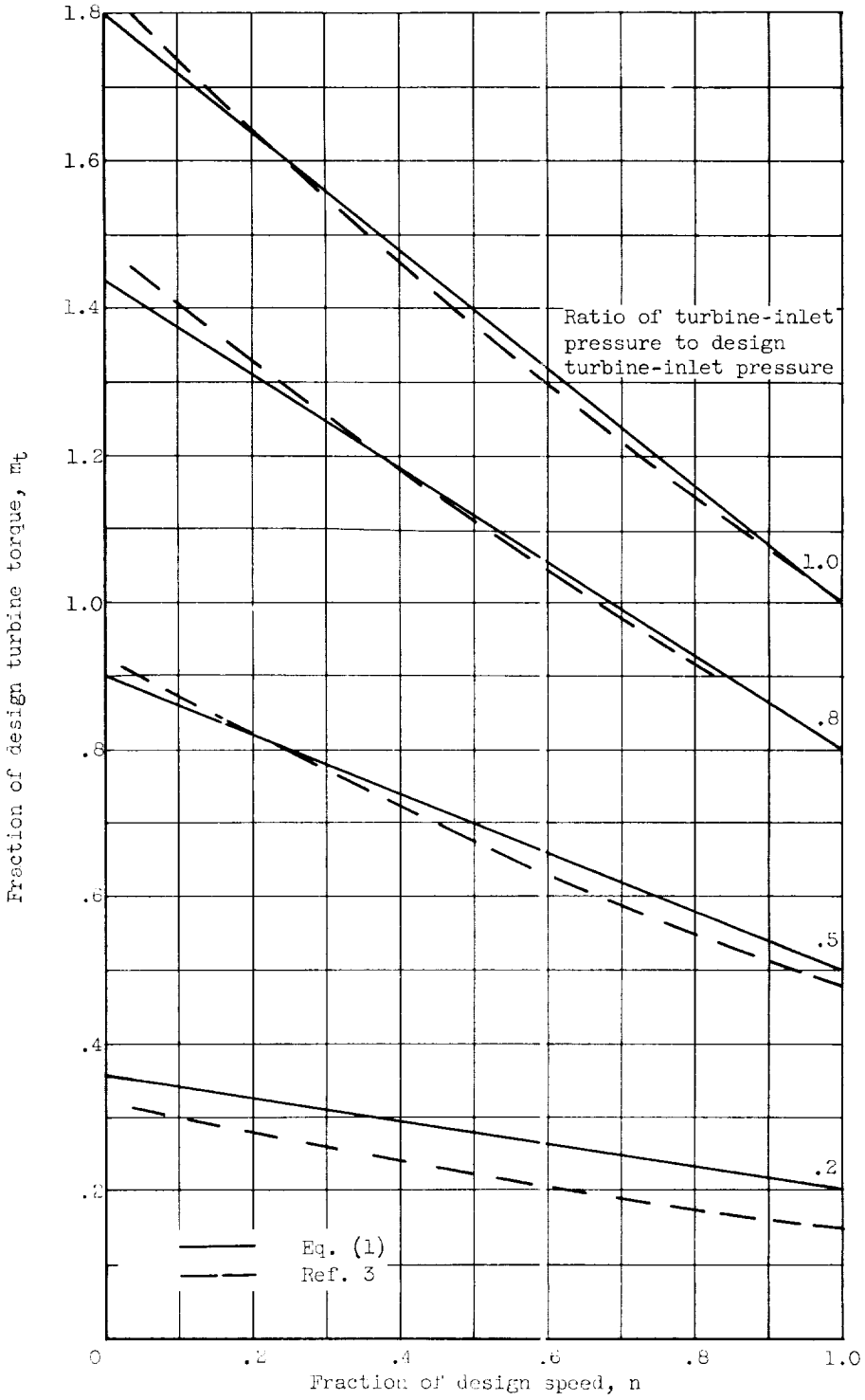

Figure 3. - Comparison of torque-speed relations assumed from equation (1) with those derived from reference 3 for several ratios of turbine-inlet pressure to design turbine-inlet pressure.

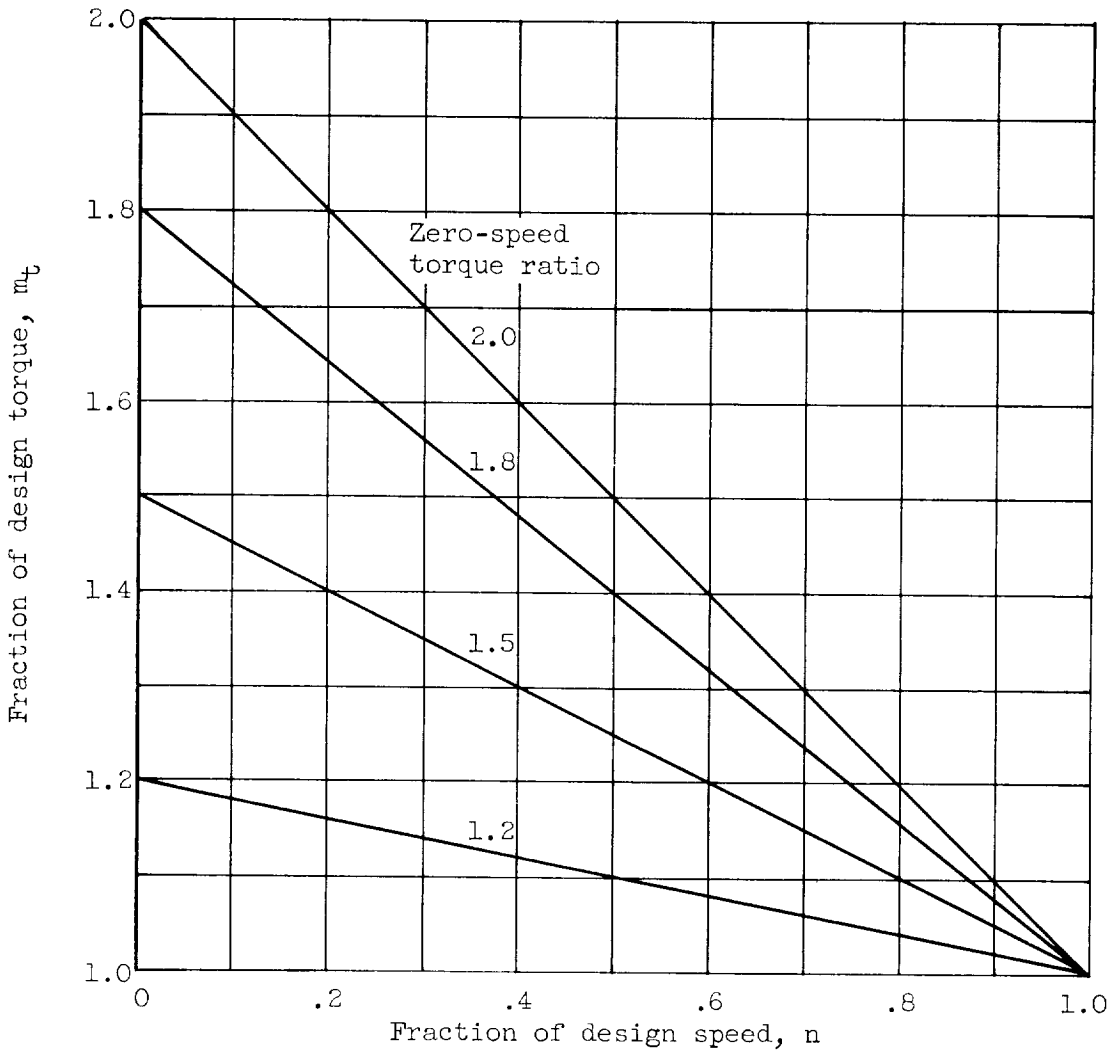

Figure 6. - Torque-speed relations for several turbine designs as computed from equation (1).

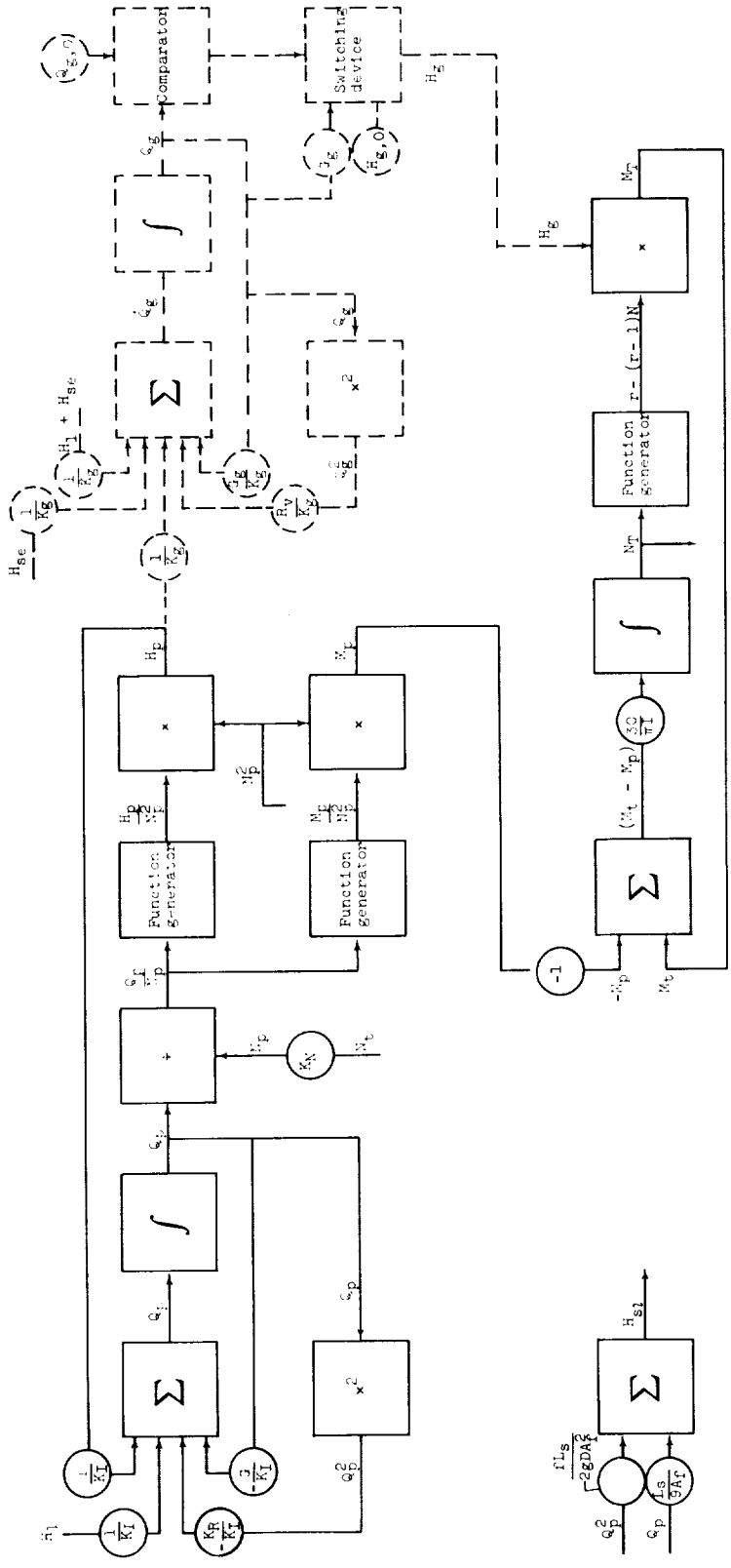

Figure 7. - Block diagram representing system equations.

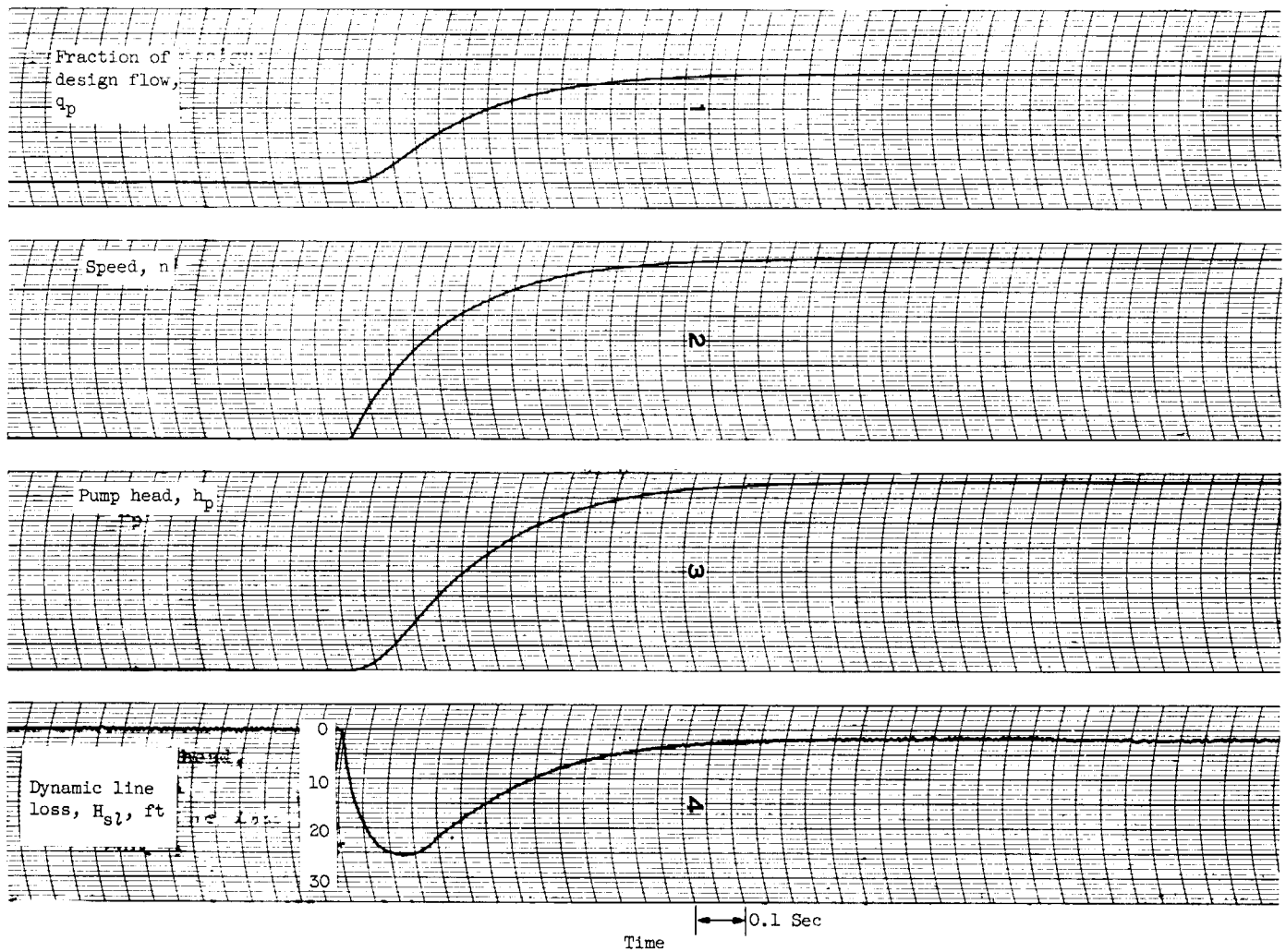

(a) Oscillograph traces.

Figure 8. - Typical starting transients for first configuration with constant-pressure turbine.

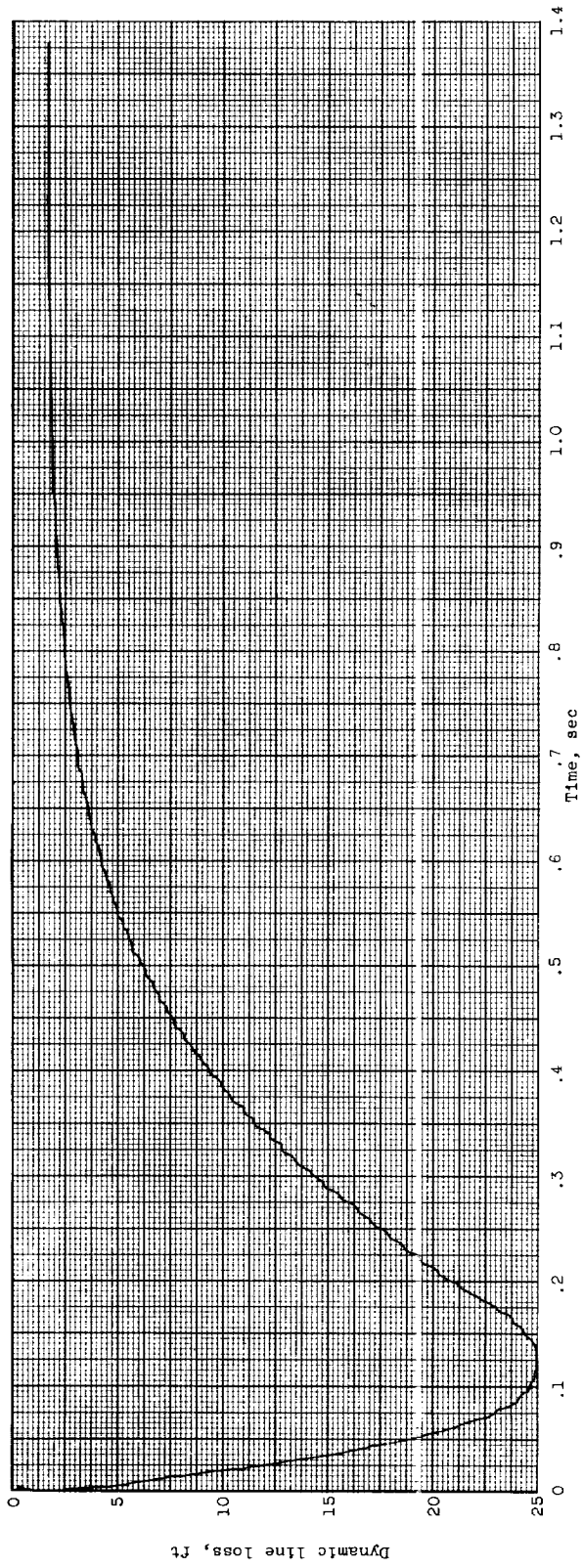

(b) Dynamic-line-loss trace.

Figure 8. - Concluded. Typical starting transients for first configuration with constant-pressure turbine.

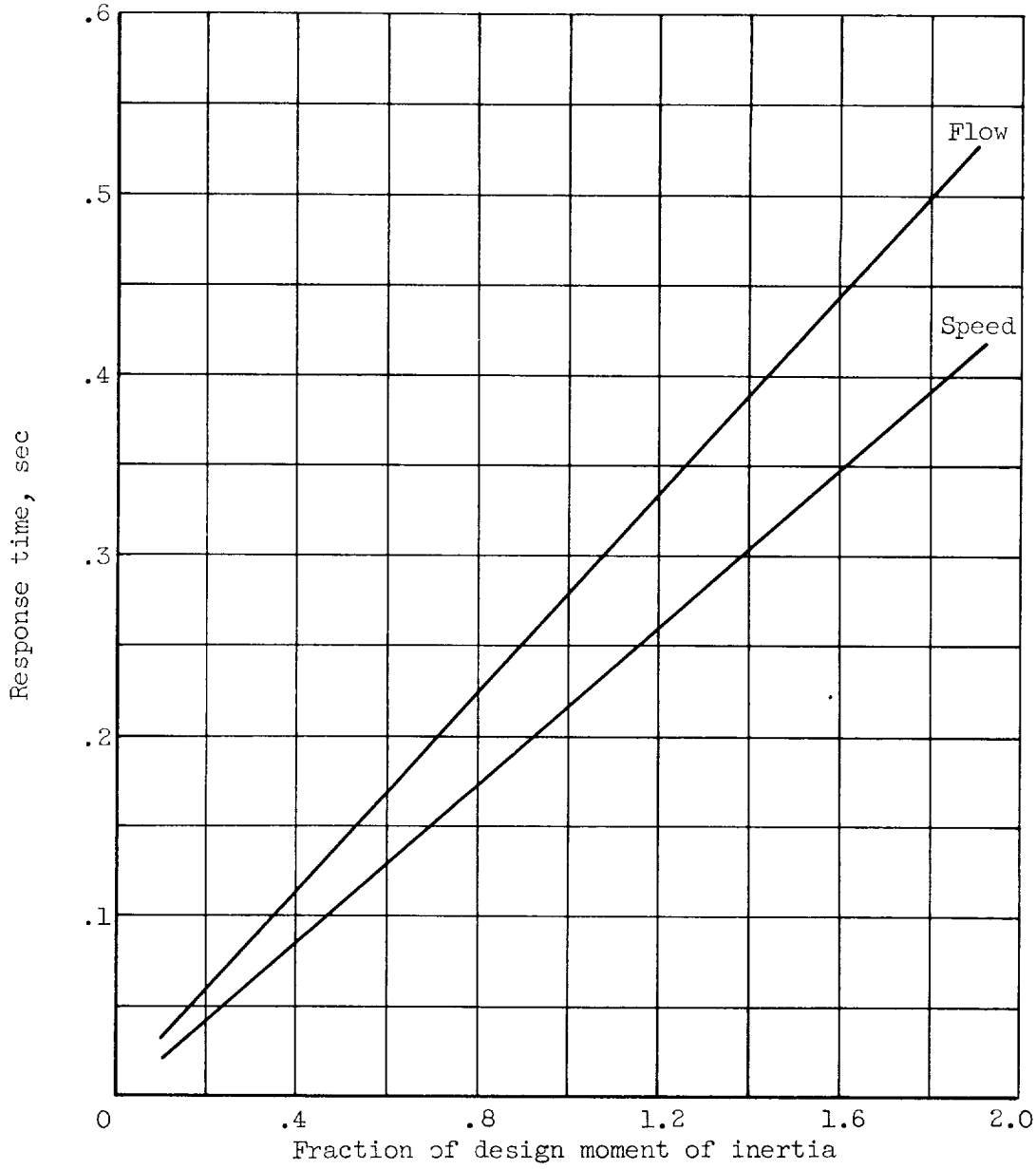

Figure 9. - Effect of turbopump moment of inertia on flow and speed response times.

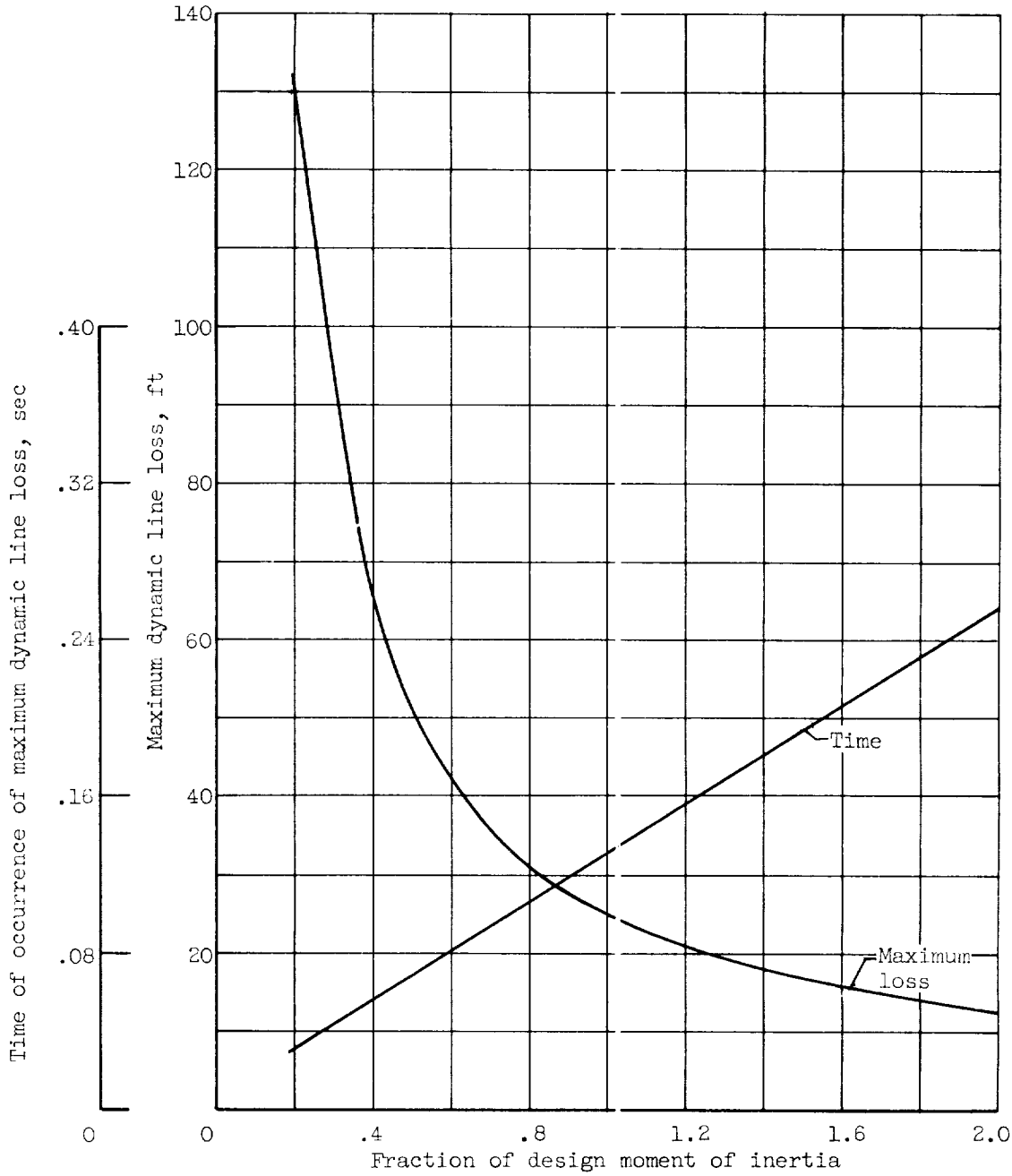

Figure 10. - Effect of turbopump moment of inertia on magnitude and time of occurrence of maximum dynamic line loss.

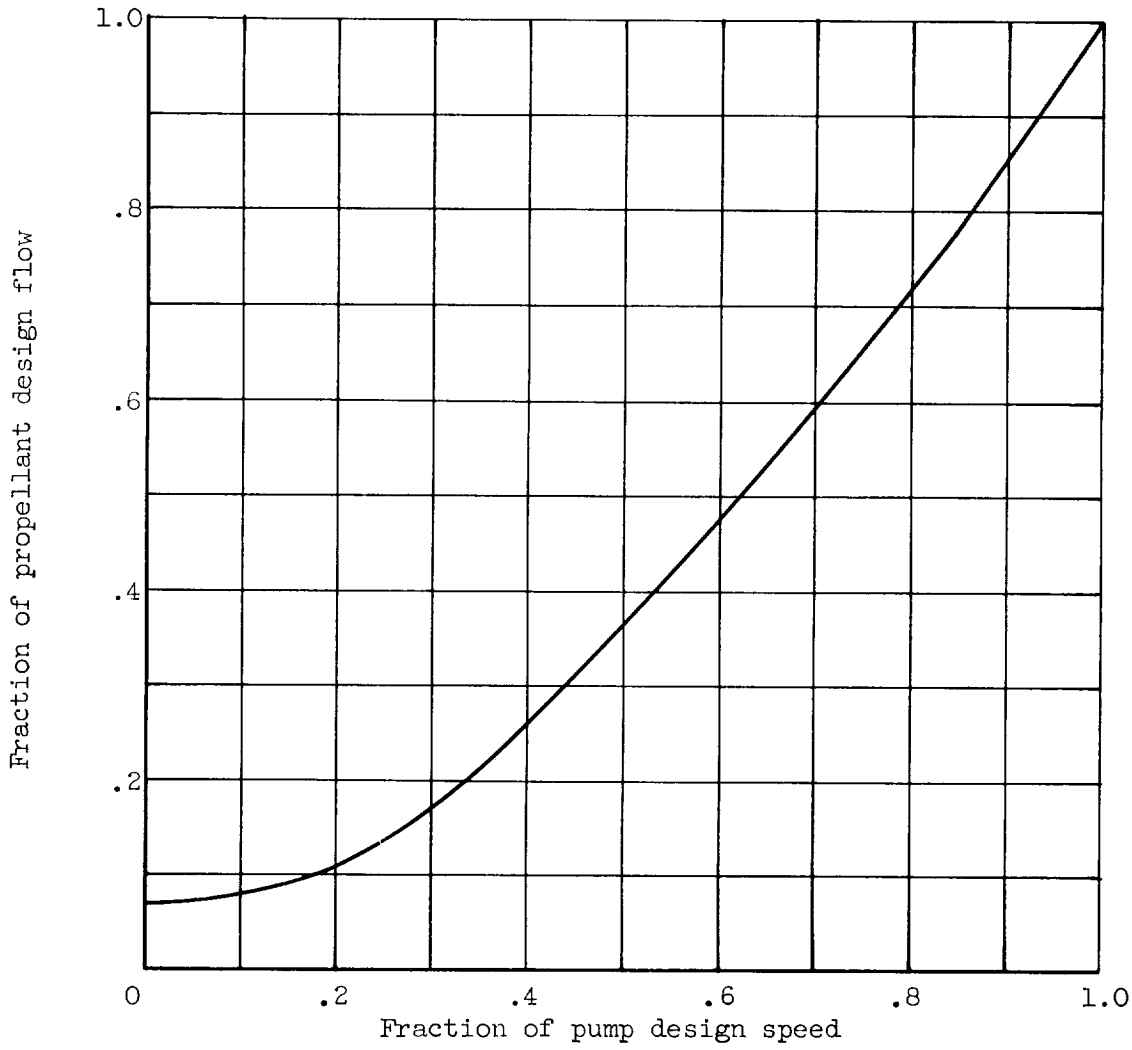

Figure 11. - Relation between propellant flow and pump rotational speed during starting transient. All parameter values nominal.

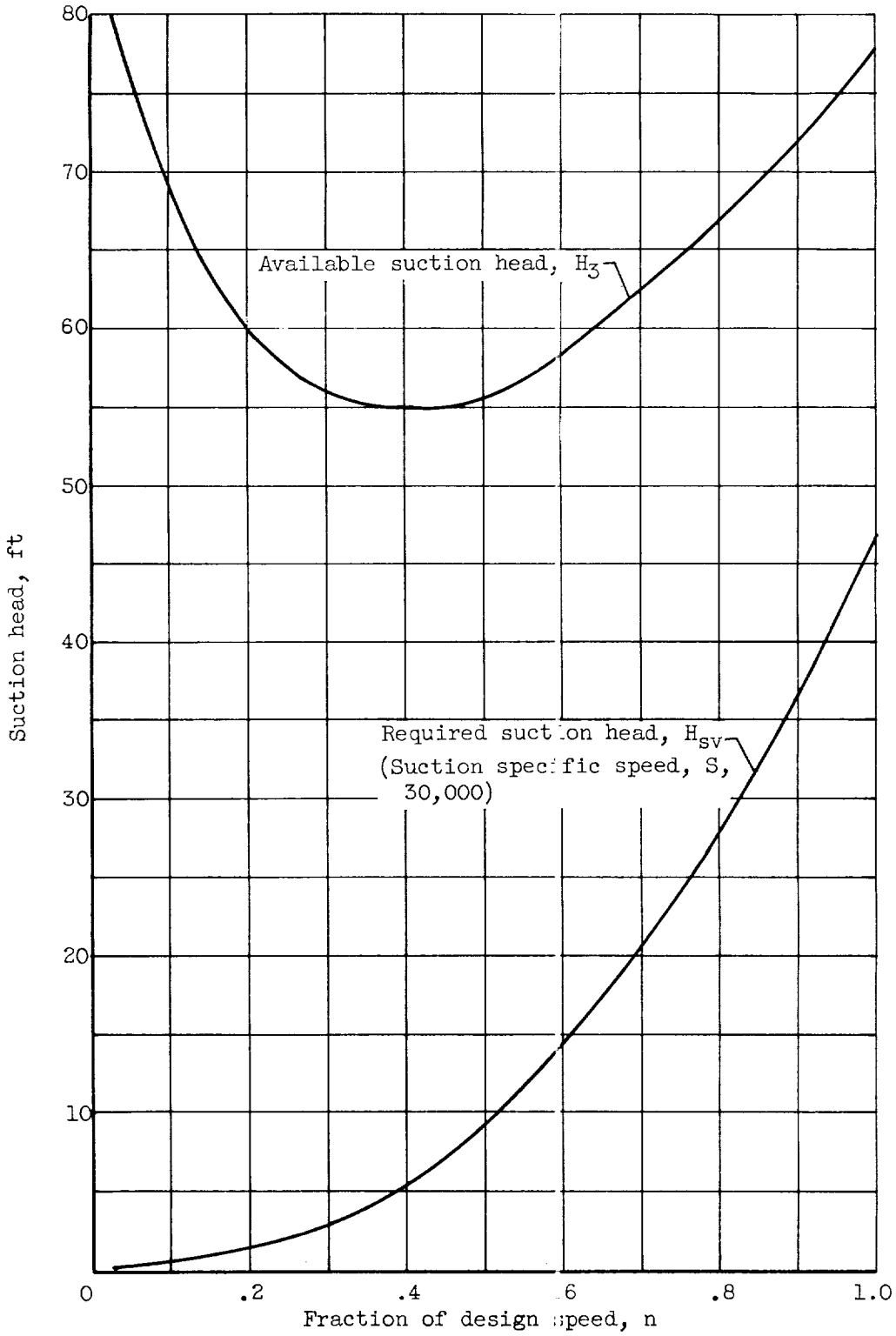

Figure 12. - Comparison of available and required suction heads for nominal configuration.

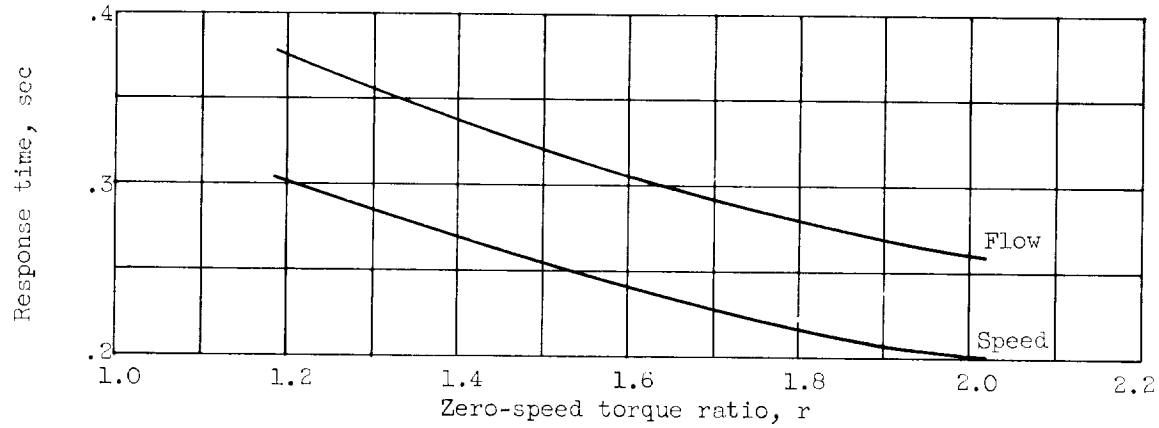

Figure 13. - Effect of turbine zero-speed torque ratio on flow and speed response times. Turbopump moment of inertia, 0.28 (lb)(ft)(sec^2).

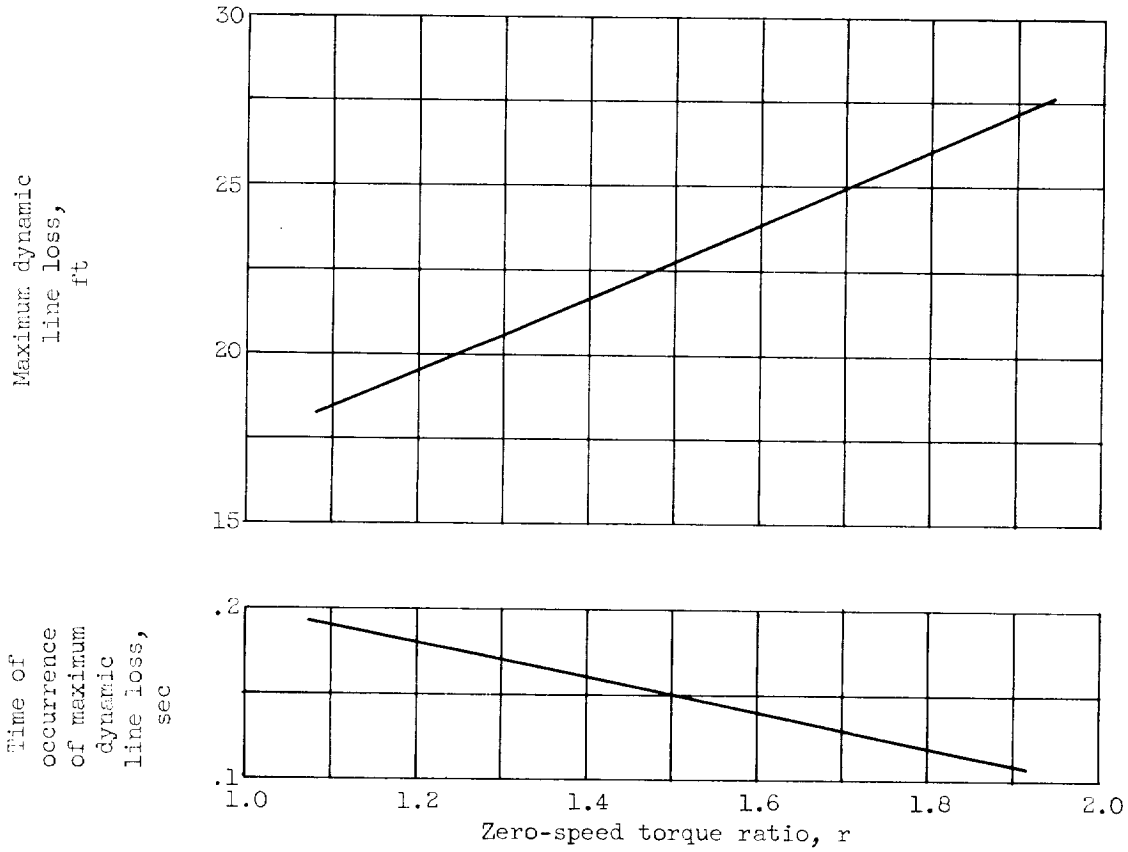

Figure 14. - Effect of turbine zero-speed torque ratio on magnitude and time of occurrence of maximum dynamic line loss. Turbopump moment of inertia, 0.28 (lb)(ft)(sec^2).

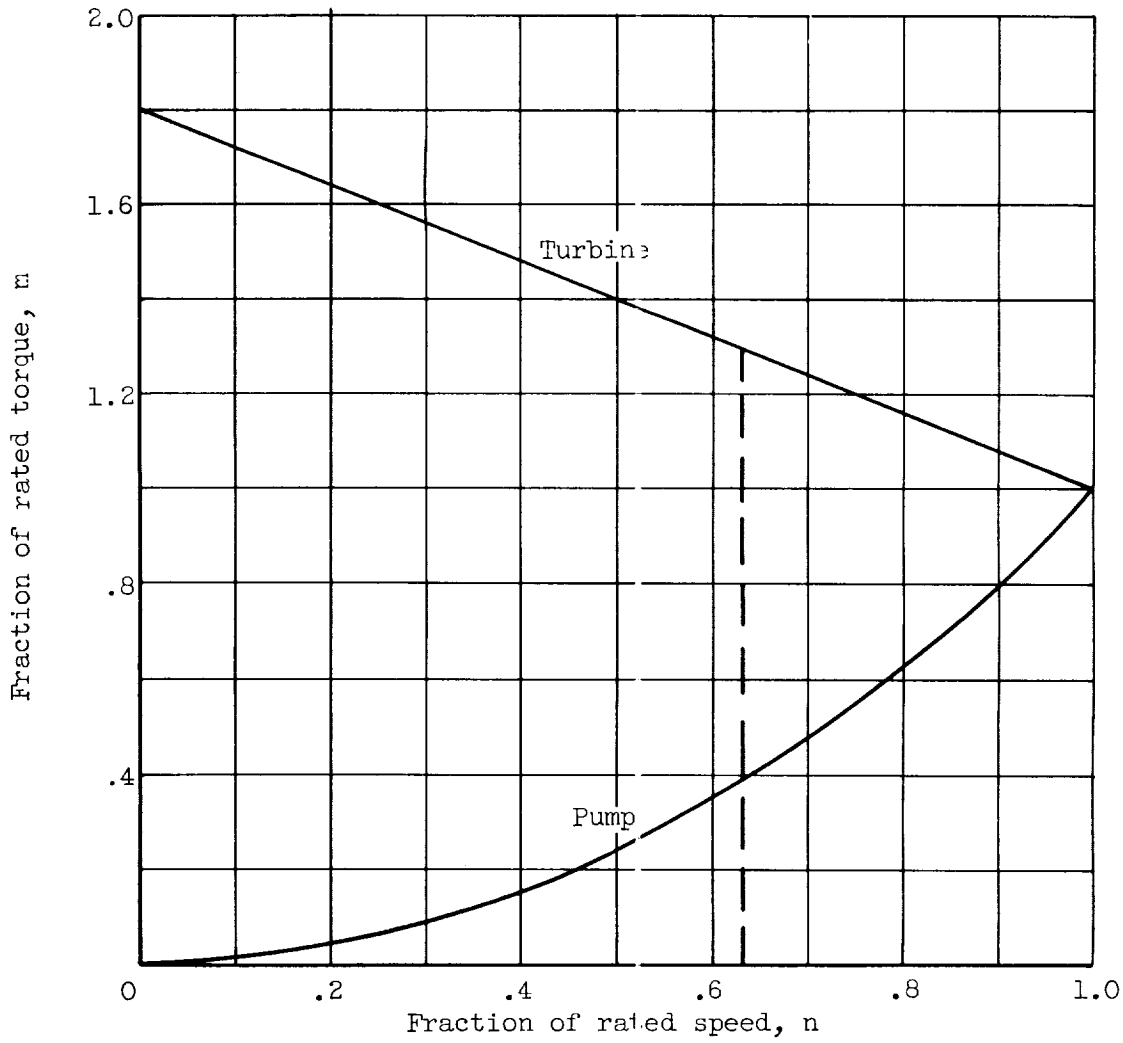

Figure 15. - Comparison of turbine torque available with pump torque required.

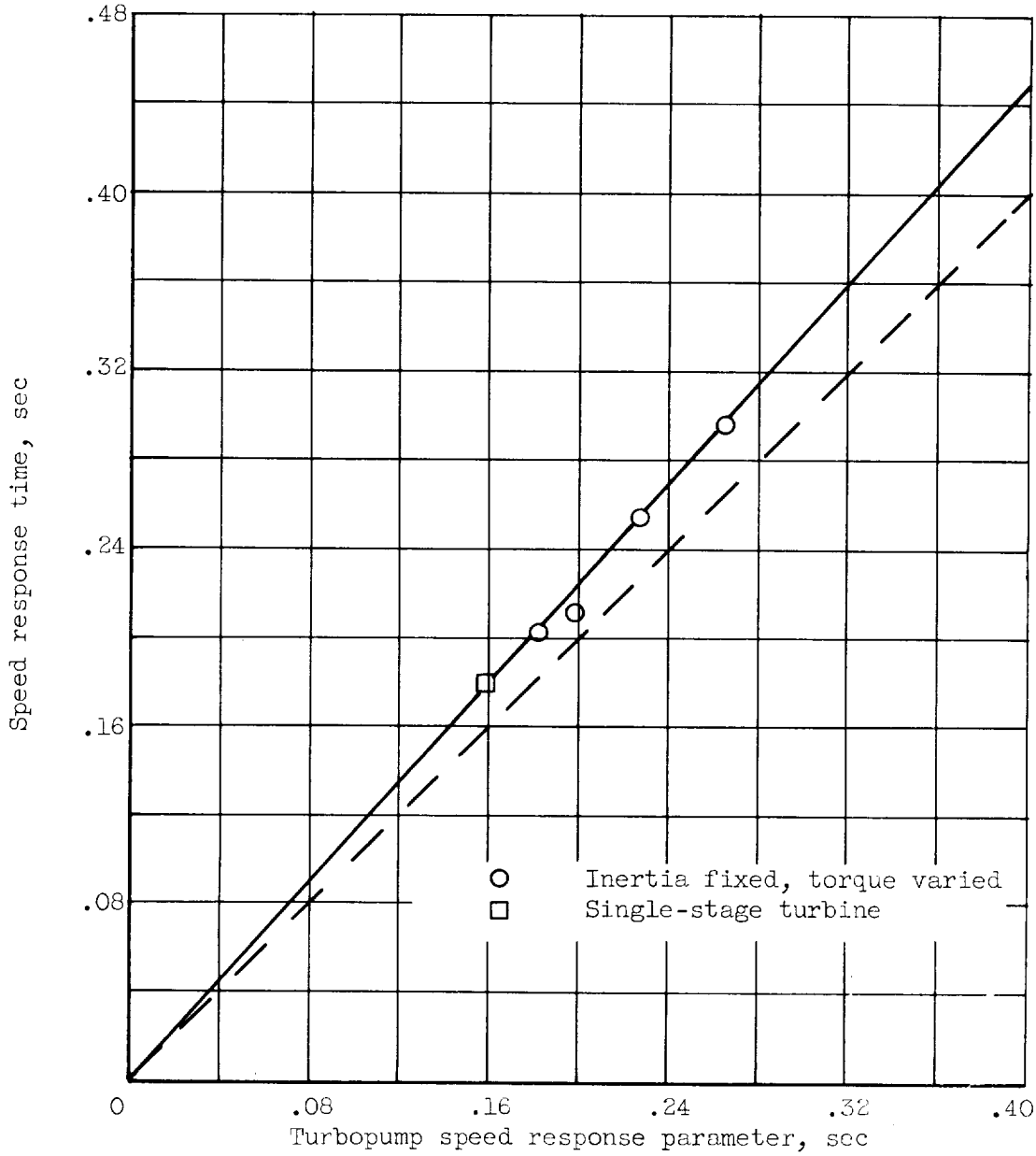

Figure 18. - Correlation between turbopump speed response parameter and speed response time.

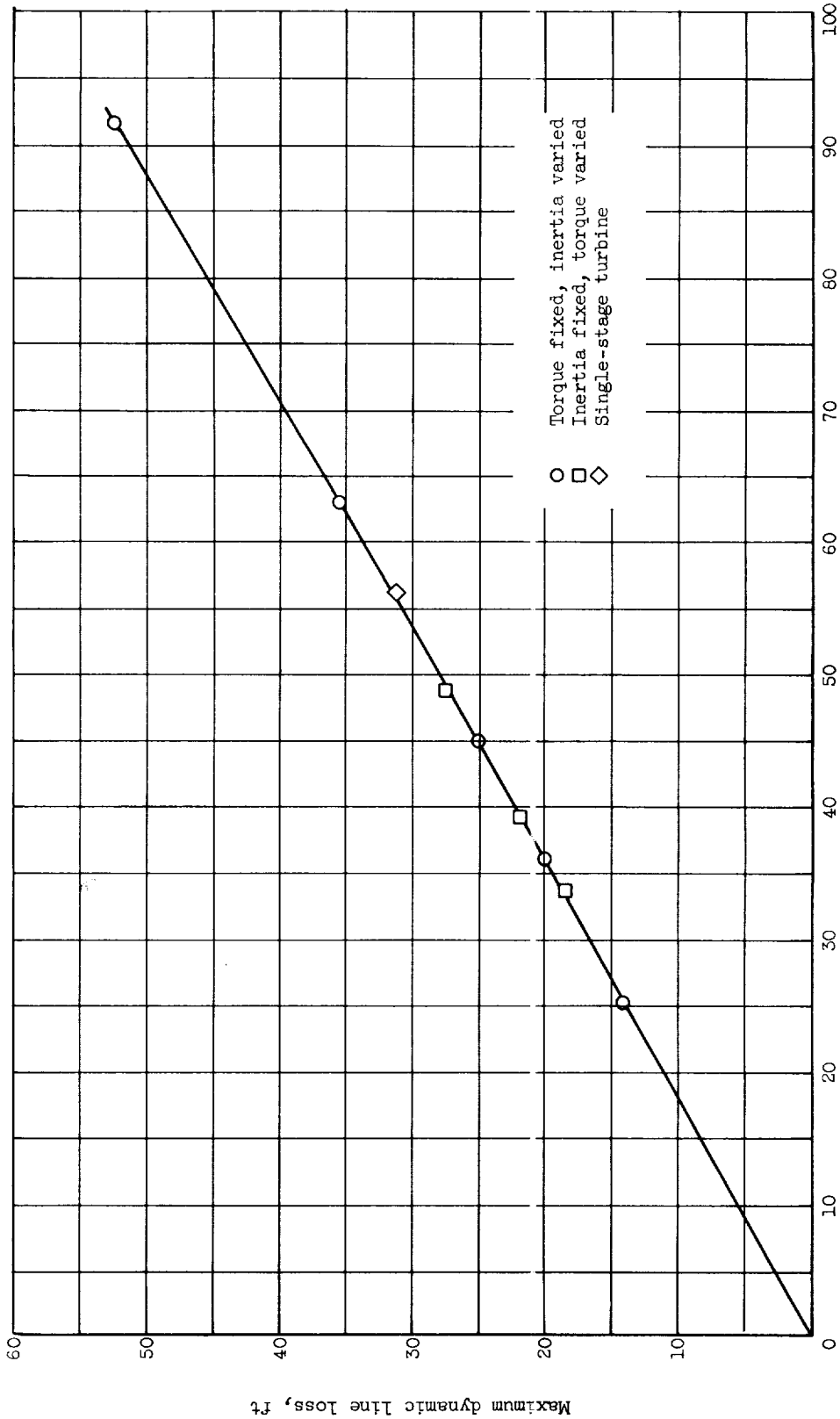

Figure 17. - Correlation between maximum dynamic line loss and maximum-dynamic-line-loss parameter.

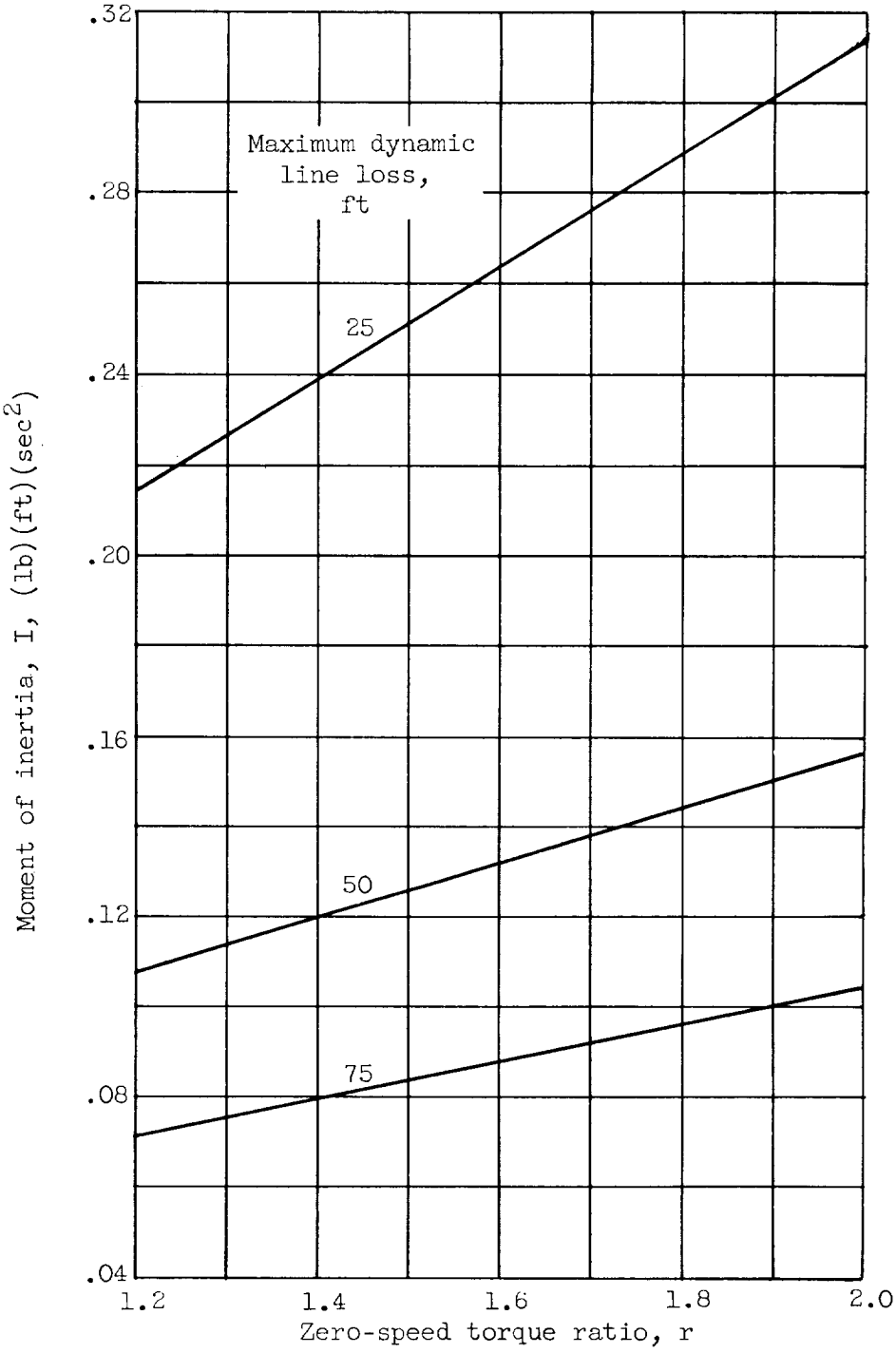

Figure 18. - Calculated relation between turbopump moment of inertia and turbine zero-speed torque ratio for several values of maximum dynamic line loss.

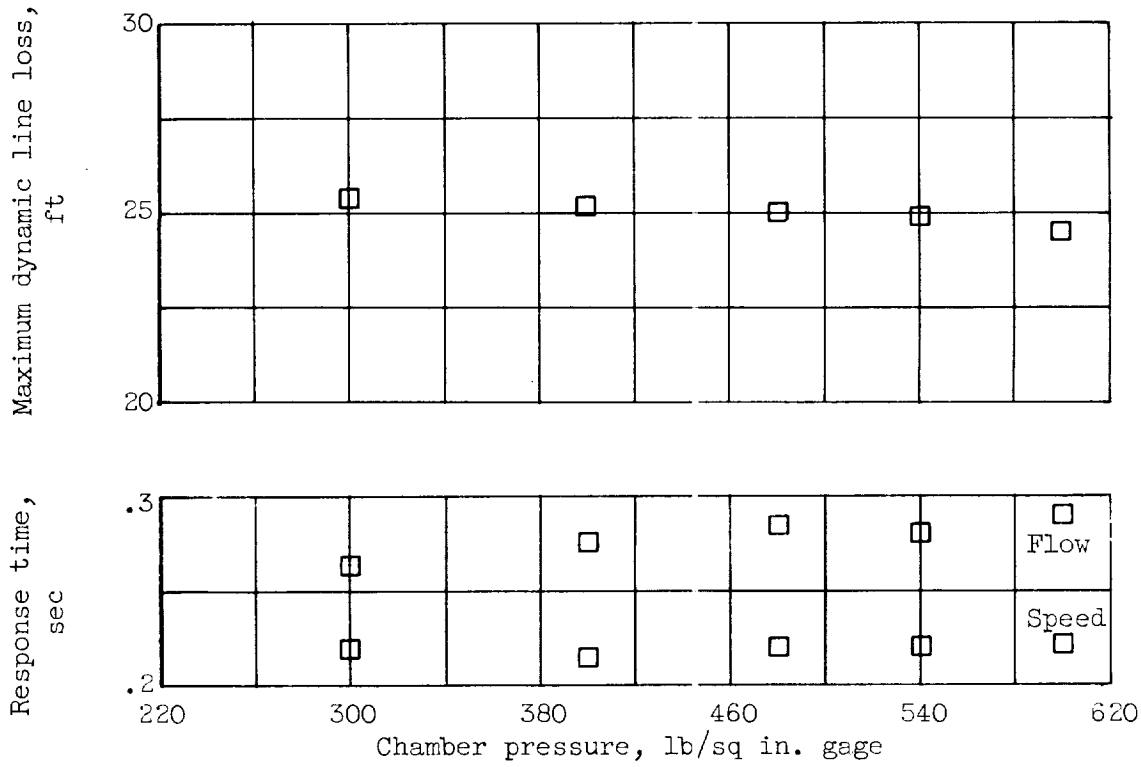

Figure 19. - Effect of rocket chamber pressure on flow and speed response times and maximum dynamic line loss. Pump head, constant; injector pressure drop, varied.

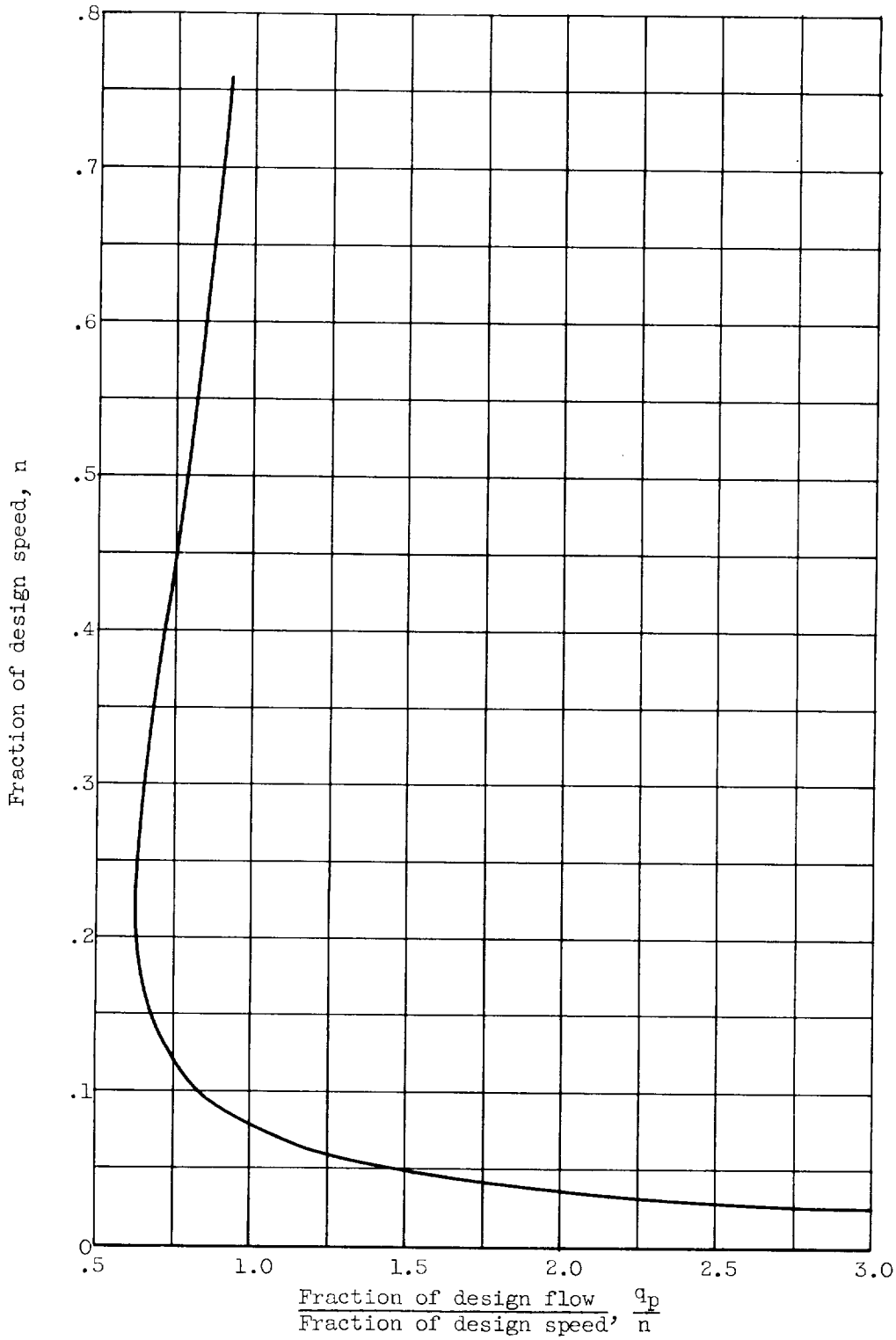

Figure 20. - Variation of $q_p/$.. for pump during starting transient.

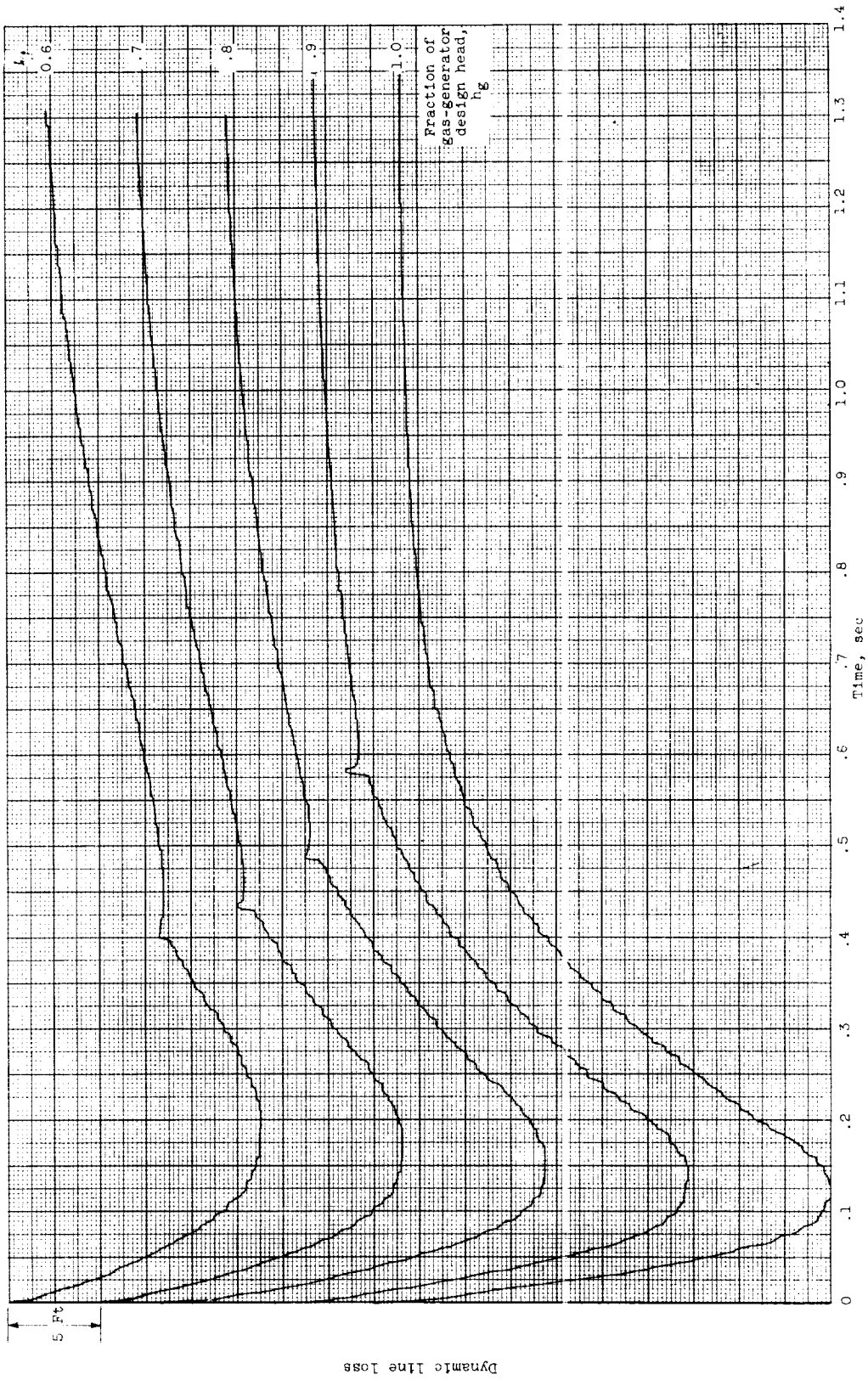

(a) Fraction of gas-generator design head from 0.6 to 1.0.

Figure 21. - Dynamic-line-loss trace for bootstrap configuration.

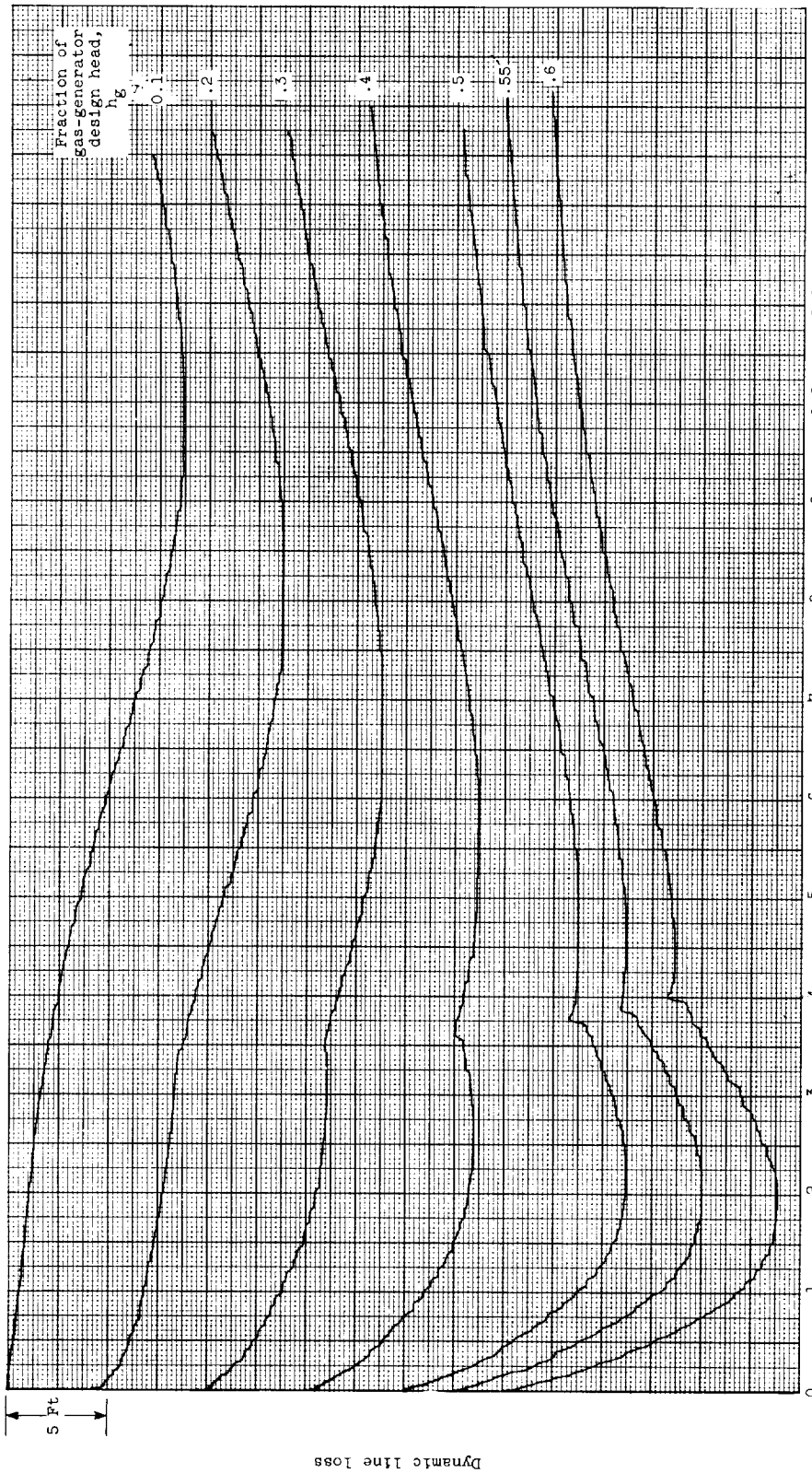

(b) Fraction of gas-generator design head from 0.1 to 0.6.

Figure 21. - Concluded. Dynamic-line-loss trace for bootstrap configuration.

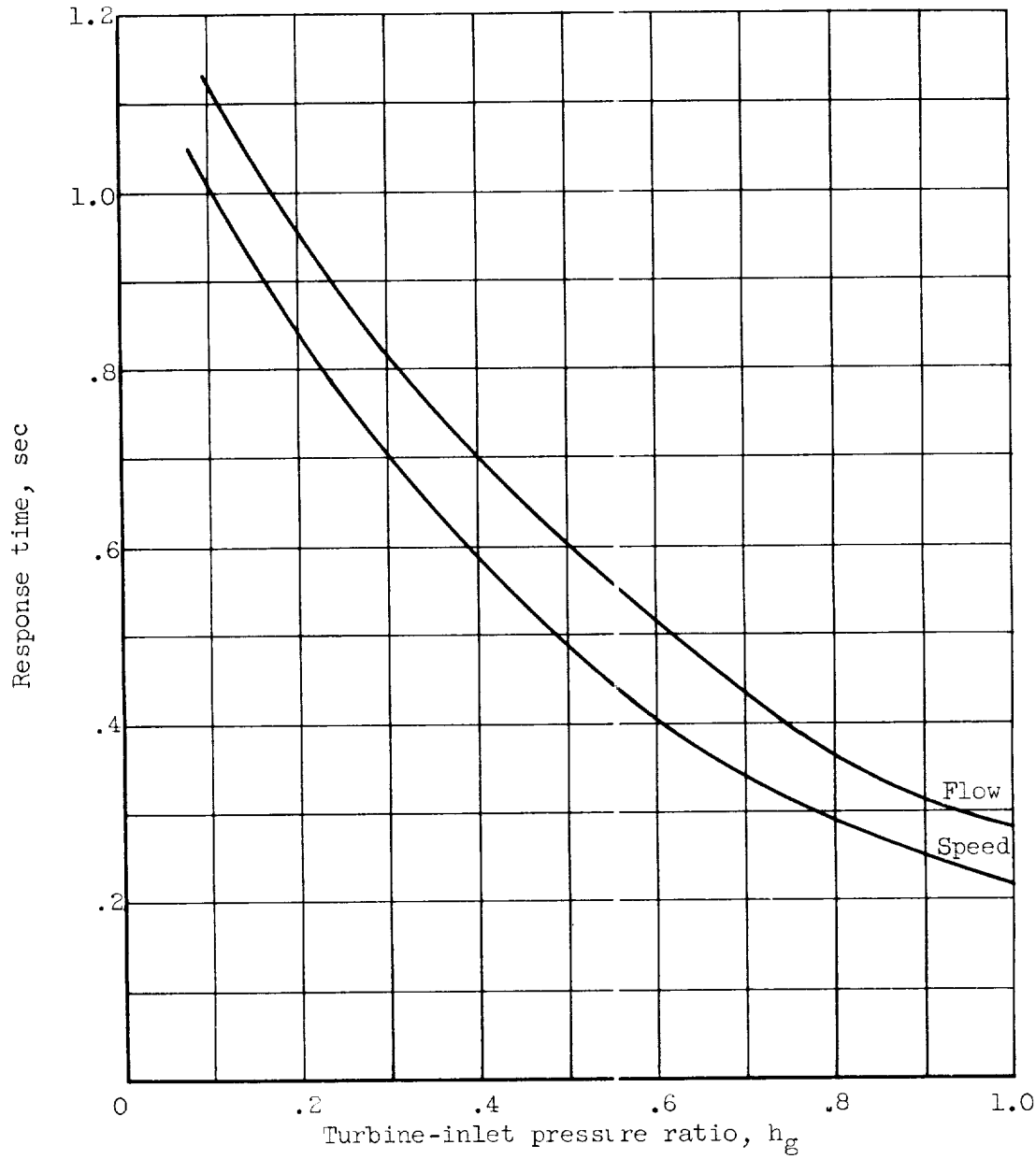

Figure 22. - Effect of turbine-inlet pressure ratio on flow and speed response times in bootstrap configuration.

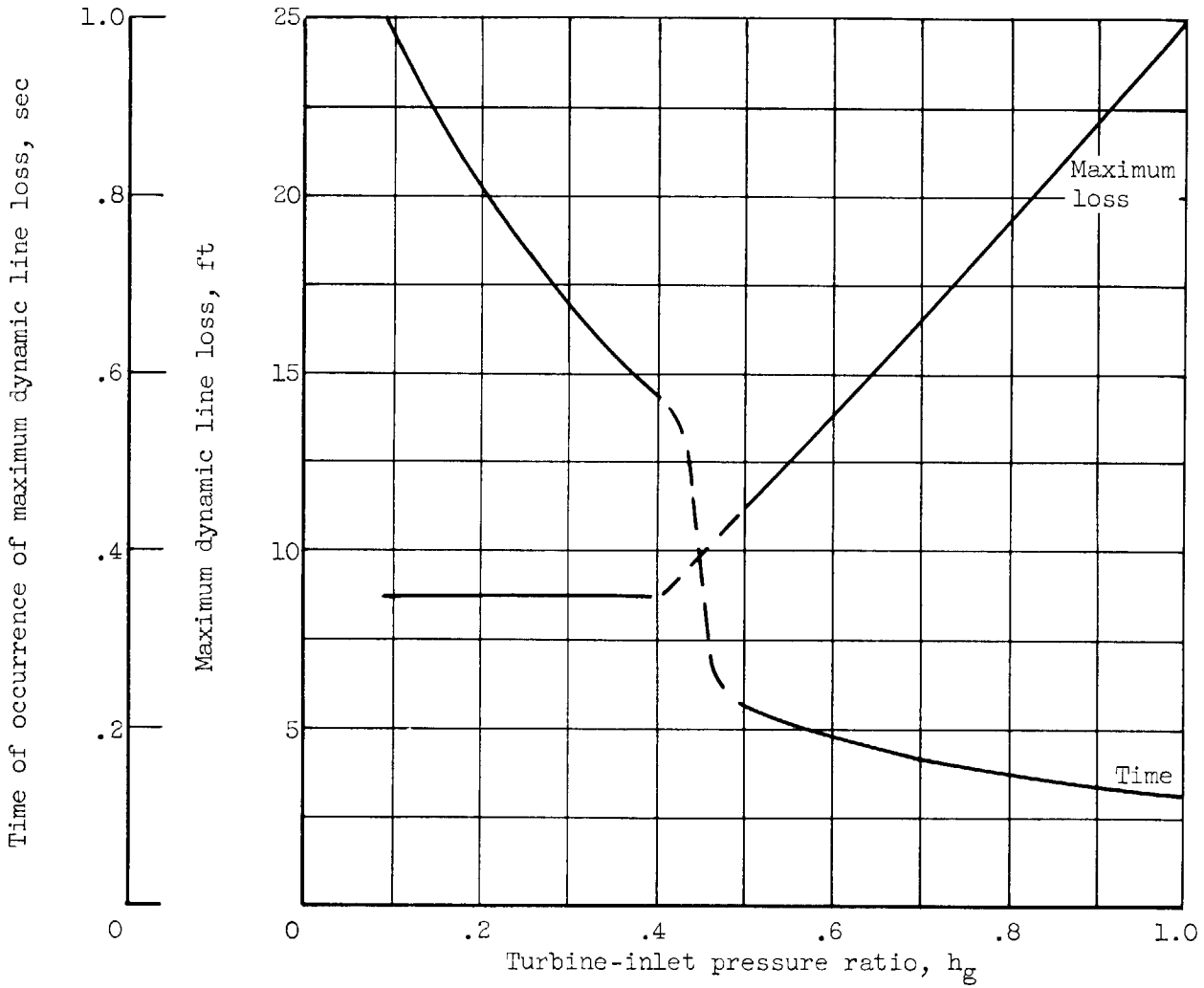

Figure 23. - Effect of turbine-inlet pressure ratio on magnitude and time of occurrence of maximum dynamic line loss in bootstrap configuration.

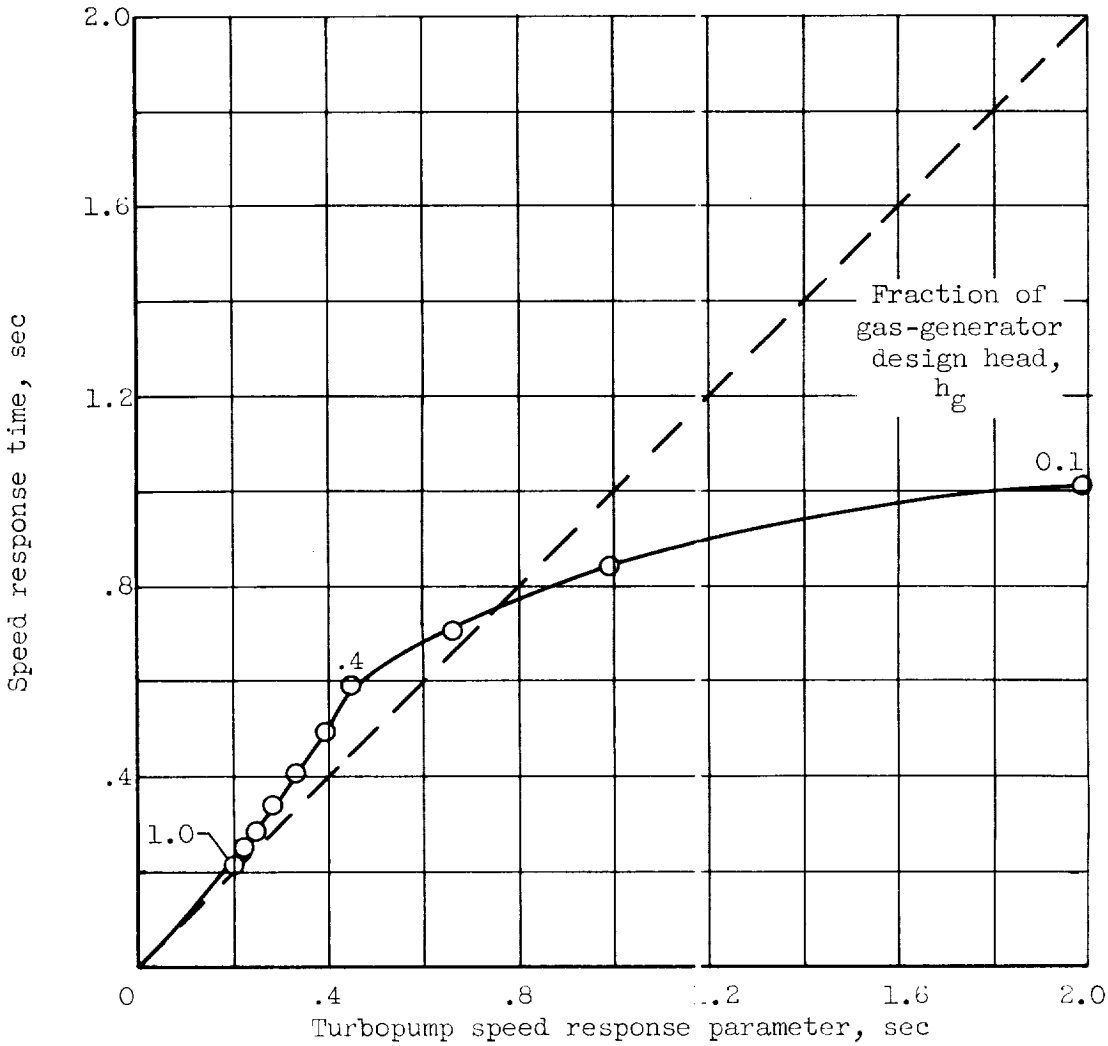

Figure 24. - Relation between speed response time and turbopump speed response parameter for bootstrap configuration.

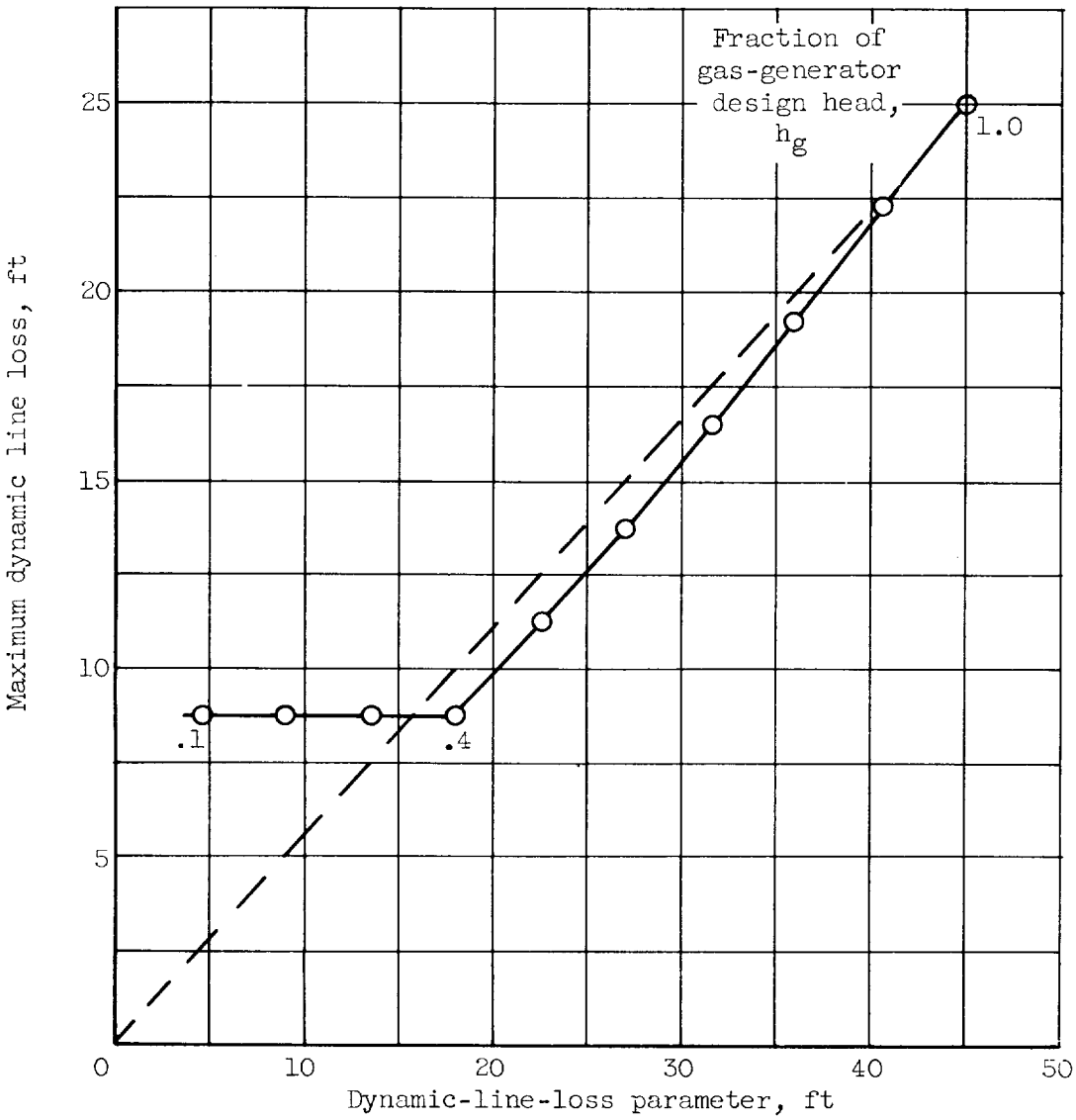

Figure 25. - Relation between maximum dynamic line loss and dynamic-line-loss parameter for bootstrap configuration.

NASA - Langley Field, Va. E-201